Local contact sub-Finslerian geometry for maximum norms in dimension 3 *

A.-L Ali, Grégoire Charlot

Local contact sub-Finslerian geometry for maximum norms in dimension 3*

Entisar A.-L. Ali♠ and G. Charlot♣

♠ *Univ. Grenoble Alpes, CNRS, Institut Fourier, F-38000 Grenoble, France*
Dyala University, Irak
entisar.ali@univ-grenoble-alpes.fr
♣ *Univ. Grenoble Alpes, CNRS, Institut Fourier, F-38000 Grenoble, France*
gregoire.charlot@univ-grenoble-alpes.fr

February 1, 2019

Abstract

Local geometry of sub-Finslerian structures in dimension 3 associated with a maximum norm are studied in the contact case. A normal form is given. Short extremals, local switching conjugate and cut loci, and small spheres are described in the generic case.

Keywords: local optimal synthesis, sub-Finslerian geometry, contact distribution.

1 Introduction

From a geometric point of view the sub-Finslerian (SF) structure we are interested in here is a triplet $(M, \Delta, |.|_\infty)$ where M is a connected manifold, Δ is a sub-bundle of the tangent bundle, and $|.|_\infty$ is a maximum norm on Δ. With such a structure we can define

Definition 1. Let $\gamma : [0, T] \to M$ be a curve in M. It is said admissible if $\dot\gamma(t) \in \Delta_{\gamma(t)}$ a.e. The length of an admissible γ is defined as

$$\ell(\gamma) := \int_0^T |\dot\gamma(t)|_\infty dt$$

and the distance between two point p and q in M as the infimum of the lengths of the curves that join p to q

$$d(p, q) = \inf\{\ell(\gamma) \,|\, \dot\gamma(t) \in \Delta_{\gamma(t)} \text{ a.e., } \gamma(0) = p, \gamma(T) = q\}.$$

If $Lie_q(\Delta) = T_qM$ for any q then locally, for any couple of points (q_1, q_2), exists an admissible curve joining q_1 and q_2. The distance between q_1 and q_2 is defined as the infimum of the lengths of the admissible curves joining the two points.

*This research has been supported by ANR-15-CE40-0018.

When one is only interested in local issues, we can define the structure by the data of k linearly independent vector fields $F_1, \cdots, F_k$ and by the standard maximum norm defined on $\text{span}(F_1, \cdots, F_k)$ by

$$|G| = \max_i \{|u_i| \ \mid G = \sum_i u_i F_i\}.$$

From a control point of view, we are considering the dynamics

$$\dot{q} = \sum_{i=1}^{k} u_i F_i(q), \tag{1}$$

with the constraints

$$|u_i| \leq 1, \forall i \leq k, \tag{2}$$

and we are interested in the optimal synthesis for the problem of minimizing time. In this situation $\Delta = \text{span}\{F_1, \cdots, F_k\}$. In this article, we are interested only in the local version of this problem, that is to understand the local synthesis for small time (or small distance). Moreover we fix our attention on the case of constant rank of smallest dimension namely $n = 3, k = 2$. In the following we work in the neighborhood of $0 \in \mathbb{R}^3$.

We say that a property is generic for this class of sub-Finslerian metrics if it is true on a residual set of such metrics for the C^∞-Whitney topology. Genericity is usually proven using Thom tranversality theorem. One proves easily that generically the set of points q where a distribution Δ of dimension 2, on a manifold of dimension 3, satisfies $[\Delta, \Delta]_q = \Delta_q$ is a sub-manifold of dimension 2 called the Martinet surface. Outside this surface, the distribution is contact: $[\Delta, \Delta]_q = T_q M$. We are interested in describing local objects, such as optimal trajectories, cut locus, conjugate locus, switching locus and small spheres at contact points.

Few publications exist about sub-Finslerian geometry since it is a new subject. Let mention the works [22, 23] for dimension 3, considering norms which are smooth outside the zero section. In [19], the sphere of a left invariant sub-Finsler structure associated to a maximum norm in the Heisenberg group is describded. In the preprint [7], the authors describe the extremals (and discuss in particular their number of switches before the loss of optimality) for the Heisenberg, Grushin and Martinet distributions. In the preprint [6], the authors describe, in the 2D generic case, the small spheres and the local cut locus. In this last preprint, the distribution is not supposed of constant rank and it can be related to the almost-riemannian case, see [2, 18, 17, 14, 16].

The work we propose here is a continuation of what has been done in sub-Riemannian geometry at the end of the nineties for codimension one distributions in the contact, quasi-contact and Martinet cases (see [1, 15, 13, 24, 4, 20]). These works, in addition to the interest of understanding the local geometry, were in particular motivated by results on the heat kernel asymptotics in the sub-Riemannian context (see [12, 26, 27, 11]). They allowed recently to give new results on the asymptotics (see [9, 8]).

In section 2, we construct a normal form for couples (F_1, F_2) defining contact distribution Δ. In section 3, we establish some properties of the minimizing trajectories and construct exponential maps. In section 4 we present the optimal synthesis of the nilpotent case. In section 5, we present the jets of the extremals, the switching and conjugate times and the switching and conjugate loci for extremals "following" the bracket $[F_1, F_2]$. In section 6, we calculate the cut locus generated by these extremals, similar to the cut locus in the 3D contact sub-Riemannian case. In section 7

we discuss the optimal synthesis linked to extremals with only one control switching several times, very different from the sub-Riemannian case. In section 8, we discuss the stability of the conjugate and cut loci constructed in the previous sections.

2 Normal form

In this section, the goal is to construct a normal form for the couple (G_1, G_2) defined by $G_1 = F_1 + F_2$ and $G_2 = F_1 - F_2$. As we will see later, $\pm G_1$ and $\pm G_2$ are the velocities of the non singular extremals of the optimal control system defined by (1) and (2).

Since we consider only points q where the distribution is contact then G_1, G_2 and $[G_1, G_2] = -2[F_1, F_2]$ form a basis of $T_q\mathbb{R}^3$. Hence, we can build a coordinate system centered at q, by the following way. Let denote e^{tX} the flow at time t of a vector field X. We can define

$$\Xi : (x, y, z) \longmapsto \mathrm{e}^{xG_1}\mathrm{e}^{yG_2}\mathrm{e}^{z[G_1,G_2]}q,$$

which to (x, y, z) associates the point reached by starting at q and following $[G_1, G_2]$ during time z, then G_2 during time y and finally G_1 during time x. The map Ξ is smooth and satisfies

$$\frac{\partial \Xi}{\partial x}(x, y, z) = G_1, \quad \frac{\partial \Xi}{\partial y}(0, y, z) = G_2, \quad \text{and} \quad \frac{\partial \Xi}{\partial z}(0, 0, z) = [G_1, G_2].$$

As a consequence Ξ is not degenerate at $(0, 0, 0)$ and defines a coordinate system in a neighborhood of q. Such coordinates are called *normal coordinates* and G_1 and G_2 satisfy

$$\begin{aligned} G_1(x, y, z) &= \partial_x, \\ G_2(x, y, z) &= x\epsilon_x(x, y, z)\partial_x + (1 + x\epsilon_y(x, y, z)))\partial_y + x(1 + \epsilon_z(x, y, z))\partial_z \end{aligned}$$

where ϵ_x, ϵ_y, ϵ_z are smooth functions satisfying $\epsilon_x(0, 0, z) = \epsilon_y(0, 0, z) = \epsilon_z(0, 0, z) = 0$. Hence we can give the following expressions of G_2

$$\begin{aligned} G_2(x, y, z) = {} & (a_{200}x^2 + a_{110}xy + x\theta_x(x, y, z))\partial_x \\ & + (1 + b_{200}x^2 + b_{110}xy + x\theta_y(x, y, z))\partial_y \\ & + (x + c_{200}x^2 + c_{110}xy + c_{300}x^3 \\ & \quad + c_{210}x^2y + c_{120}xy^2 + x\theta_z(x, y, z))\partial_z \end{aligned}$$

where θ_x, θ_y and θ_z are smooth functions such that $\theta_x(0, 0, z) = \theta_y(0, 0, z) = \theta_z(0, 0, z) = 0$ and whose Taylor series of respective order $1, 1, 2$ are null with x and y of order 1 and z of order 2.

3 General facts about the computation of the optimal synthesis

In the following of the paper we are going to study the local geometry for a generic class of 3D sub-Finslerian metric defined by a maximum norm, that is for a residual set for the Whitney C^∞ topology on the set of such metrics. But, for this residual set of metrics, we are going to consider the local geometry only at points in the complementary of a set included in a finite union of codimension 1 submanifolds.

For example, we consider only contact points and generically the set of points where the distribution is not contact is the Martinet surface which has codimension 1. We may also ask that an invariant appearing in the normal form is not null, which happens also outside a codimension 1 submanifold. All along the paper we will assume only a finite number of such assumptions.

3.1 Controllability and existence of minimizers

The contact hypothesis is

$$\text{span}(F_1, F_2, [F_1, F_2]) = \mathbb{R}^3.$$

Hence, as a consequence of Chow-Rashevski theorem (see [5, 28, 21]), such a control system is locally controllable that is locally, for any two points, always exists an admissible curve joining the two points.

Moreover, since at each point the set of admissible velocities is convex and compact (in the control version), thanks to Filippov theorem (see [5, 25]), locally for any two points, always exists at least a minimizer.

3.2 Pontryagin Maximum Principle (PMP) and Switching Function

The Pontryagn Maximum Principle (PMP) gives necessary conditions for a curve to be a minimizer of the SF distance. For our problem it takes the following form.

Theorem 2 (PMP)**.** *Let define the Hamiltonian:*

$$H(q, \lambda, u, \lambda_0) = u_1 \lambda.F_1(q) + u_2 \lambda.F_2(q) + \lambda_0$$

where $q \in \mathbb{R}^3$, $\lambda \in T^*\mathbb{R}^3$, $u \in \mathbb{R}^2$ and $\lambda_0 \in \mathbb{R}_-$. For any minimizer $(q(t), u(t))$ there exist a never vanishing Lipschitz continuous covector $\lambda : t \mapsto \lambda(t) \in T^*\mathbb{R}^3$ and a constant $\lambda_0 \leq 0$ such that for a.e. $t \in [0, T]$ we have

i. $\dot{q}(t) = \frac{\partial H}{\partial \lambda}(q(t), \lambda(t), u(t), \lambda_0)$,

ii. $\dot{\lambda}(t) = -\frac{\partial H}{\partial q}(q(t), \lambda(t), u(t), \lambda_0)$,

iii. $H(q(t), \lambda(t), u(t), \lambda_0) = \max_v \{H(q(t), \lambda(t), v, \lambda_0) \mid \max_{i=1,2} |v_i| \leq 1\}$,

iv. $H(q(t), \lambda(t), u(t), \lambda_0) = 0$.

If $\lambda_0 = 0$ then q is said abnormal, if not q is said normal. It may be both. A solution of the PMP is called an extremal.

Remark 3. It is well known that for a contact distribution there is no abnormal extremal. In the following we fix $\lambda_0 = -1$.

In the following, we will have to consider the vector fields $F_3 = [F_1, F_2]$, $F_4 = [F_1, [F_1, F_2]]$ and $F_5 = [F_2, [F_1, F_2]]$. We can now define

Definition 4. For an extremal triplet $(q(.), \lambda(.), u(.))$, we define the functions

$$\phi_i(t) =< \lambda(t), F_i(q(t)) >, i = 1 \cdots 5.$$

The functions ϕ_1 and ϕ_2 are called the switching functions.

Proposition 5. *For $i = 1, 2$*

1. *If $\phi_i(t) > 0$ (resp $\phi_i(t) < 0$) then $u_i(t) = 1$ (resp $u_i(t) = -1$).*

2. *If $\phi_i(t) = 0$ and $\dot{\phi}_i(t) > 0$ (resp $\dot{\phi}_i(t) < 0$) then ϕ_i changes sign at time t and the control u_i switches from -1 to $+1$(resp from $+1$ to -1).*

Proof: Point 1. is a direct consequence of the maximality condition of the PMP. Point 2. is a direct consequence of point 1.

Remark 6. One can computes easily that along a bang arc

$$\dot{\phi}_1 = -u_2\phi_3 \qquad \text{and} \qquad \dot{\phi}_2 = u_1\phi_3.$$

and moreover, since (F_1, F_2, F_3) is a frame of the tangent space, we can define the function f_{ij} for $i = 4, 5$ and $j = 1, 2, 3$ by setting

$$F_4 = [F_1, [F_1, F_2]] = f_{41}F_1 + f_{42}F_2 + f_{43}[F_1, F_2],$$

$$F_5 = [F_2, [F_1, F_2]] = f_{51}F_1 + f_{52}F_2 + f_{53}[F_1, F_2].$$

Now, along an extremal, one computes easily that

$$\begin{aligned} \dot{\phi}_3 &= u_1\phi_4 + u_2\phi_5 &(3)\\ &= u_1(f_{41}\phi_1 + f_{42}\phi_2 + f_{43}\phi_3) + u_2(f_{51}\phi_1 + f_{52}\phi_2 + f_{53}\phi_3) &(4)\end{aligned}$$

Definition 7. We call *bang* an extremal trajectory corresponding to constant controls with value 1 or -1 and *bang-bang* an extremal which is a finite concatenation of bangs. We call *u_i-singular* an extremal corresponding to a null switching function $\phi_i(.)$. A time t is said to be a *switching time* if u is not bang in any neighborhood of t.

Remark 8. Notice that the switching functions $\phi_i(.)$ are at least Lipschitz continuous. Moreover thanks to condition 4 of PMP and $\lambda_0 = -1$ we have that $u_1(t)\phi_1(t) + u_2(t)\phi_2(t) = 1$, for all t which implies

$$|\phi_1(t)| + |\phi_2(t)| = 1.$$

Remark 9. Along a u_1-singular, $\phi_1 \equiv 0$, $\phi_3 \equiv 0$ and $|\phi_2| \equiv 1$. If $\phi_2 \equiv \pm 1$ then $u_2 \equiv \pm 1$ and, thanks to equation (4), we get that

$$u_1 f_{42} \pm f_{52} \equiv 0.$$

which determines entirely the control u_1.

3.3 Change of coordinates

We first concentrate our attention on extremals with initial $|\lambda_z|$ very large corresponding to short cut times (as we will see later).

Following the techniques used in the 3d-contact case in sub-Riemannian geometry (see Agrachev et al [3]), one can make the following change of coordinates and time

$$r = \frac{1}{\lambda_z}, \quad s = \frac{t}{r}, \quad p_x = r\lambda_x, \quad p_y = r\lambda_y.$$

Denoting $p = (p_x, p_y, 1)$ and $q = (x, y, z)$ one gets the equations for the extremals

$$\begin{aligned}
\frac{dq}{ds} &= r(u_1 F_1(q) + u_2 F_2(q)), \\
\frac{dp}{ds} &= r(-p(u_1 dF_1(q) + u_2 dF_2(q)) + (p(u_1 \frac{\partial F_1(q)}{\partial z} \\
&\quad + u_2 \frac{\partial F_2(q)}{\partial z}))p), \\
\frac{dr}{ds} &= r^2 p(u_1 \frac{\partial F_1(q)}{\partial z} + u_2 \frac{\partial F_2(q)}{\partial z}).
\end{aligned}$$

3.4 Exponential map and conjugate locus

The set of initial condition is determined by

$$H = u_1 \lambda(0) F_1(0) + u_2 \lambda(0) F_2(0) - 1 = 0$$

which implies $\max\{|\lambda_x(0)|, |\lambda_y(0)|\} = 1$. This implies that $\max\{|p_x(0)|, |p_y(0)|\} = r(0)$.

If an extremal is not singular, then it starts by a first bang and hence by the speed $\pm G_1$ or $\pm G_2$. Assume $r_0 > 0$. If the first bang follows $\pm G_1$ then $p_x(0) = \pm r_0$ and we define α_2 by setting $p_y(0) = \mp r_0 \alpha_2$ with $\alpha_2 \in]-1, 1]$. If the first bang follows $\pm G_2$ then $p_y(0) = \pm r_0$ and we define α_1 by setting $p_x(0) = \pm r_0 \alpha_1$ with $\alpha_1 \in]-1, 1]$. With this convention, among the extremals starting with r_0 fixed and following $\pm G_1$ (resp $\pm G_2$), the last one to switch is the one with initial condition $\alpha_2 = 1$ (resp. $\alpha_1 = 1$).

We can hence define 4 exponential maps corresponding to the 4 initial speed $\pm G_1$ and $\mp G_2$ and describing the bang-bang extremals. For these maps, depending on r_0, α_i and s, when $\alpha_i \neq 1$ and when s is not a switching time of the extremal with initial condition (r_0, α_i), one can compute the jacobian with respect to the parameters (r_0, α_i, s).

Recall that we denote by t the time and s the new time after reparameterization.

Definition 10. The first conjugate time along an extremal is the infimum of the times t such that exist t_1 and t_2 with $0 < t_1 < t_2 < t$ such that $Jac(t_1)Jac(t_2) < 0$. The first conjugate point along an extremal is the point reached at first conjugate time and the first conjugate locus is the set of the first conjugate points.

The cut locus is the set of points where an extremal curve loses optimality.

The Maxwell set is the set of points where two optimal curves meet.

The sphere at time t is the collection of all end points at time t of the optimal extremals.

Remark 11. With this definition, it will happen that the Maxwell set is not always included in the cut locus (which is very different from the Riemannian case).

4 Nilpotent case

This part of the paper is not entirely new since this case has been studied in [7, 19]

As in sub-Riemannian geometry (see [10, 3]), the nilpotent approximation plays an important role as "good estimation" of the real situation. The nilpotent approximation at $(0, 0, 0)$ of G_1, G_2

given in the normal form is

$$\widehat{G_1} = \begin{pmatrix} 1 \\ 0 \\ 0 \end{pmatrix}, \qquad \widehat{G_2} = \begin{pmatrix} 0 \\ 1 \\ x \end{pmatrix}$$

It is a left invariant sub-Finslerian metric defined on the Heisenberg group with the representation

$$(x, y, z) \star (x', y', z') = (x + x', y + y', z + z' + xy').$$

It is the tangent space in the sense of Gromov. See [10].

The Hamiltonian for the nilpotent case is

$$H = \frac{u_1 + u_2}{2}\lambda_x + \frac{u_1 - u_2}{2}(\lambda_y + x\lambda_z) - 1.$$

Thus the differential equations are given by

$$\begin{array}{rclcrcl} \dot{x} &=& \frac{u_1+u_2}{2}, & & \dot{\lambda_x} &=& -\frac{u_1-u_2}{2}\lambda_z, \\ \dot{y} &=& \frac{u_1-u_2}{2}, & & \dot{\lambda_y} &=& 0, \\ \dot{z} &=& \frac{u_1-u_2}{2}x, & & \dot{\lambda_z} &=& 0, \end{array}$$

which implies that λ_y and λ_z are constants.

Before entering the computations, one can think that, thanks to the PMP, most of the optimal trajectories will be concatenations of bang arcs of $\pm G_1$ and $\pm G_2$. Moreover, one shows relatively easily that the extremals are solutions of an isoperimetric problem, the z coordinate being a certain area defined from the projection on the (x, y)-plane of the trajectory, as it is in the Heisenberg case in subriemannian geometry. Hence it seems clear that many optimal curves project on squares. As we will see, a large class of optimal curves satisfy this property but many others, the singular ones, do not satisfy it which is very different to the subriemannian case.

4.1 Extremals with $\lambda_z \neq 0$

Changing the variables and time for

$$r = \frac{1}{\lambda_z}, \quad s = \frac{t}{r}, \quad p_x = r\lambda_x, \quad p_y = r\lambda_y,$$

and denoting $\dot{g}$ the derivate of a function g with respect to s we have

$$\begin{array}{rclcrcl} \dot{x} &=& r\frac{u_1+u_2}{2}, & & \dot{p}_x &=& -r\frac{u_1-u_2}{2}, \\ \dot{y} &=& r\frac{u_1-u_2}{2}, & & \dot{p}_y &=& 0, \\ \dot{z} &=& r\frac{u_1-u_2}{2}x, & & \dot{r} &=& 0. \end{array}$$

Let present, for example, the computation of extremals with $\lambda_z \equiv \lambda_z(0) > 0$, $\lambda_y \equiv \lambda_y(0) = 1$, $\lambda_x \in]-1, 1]$. In x, y, z, p_x, p_y, r, s coordinates, one gets $p_y = r$, $p_x = r\alpha$ with $\alpha \in]-1, 1]$ and $\phi_1(s) = \frac{p_x(s)+p_y+x(s)}{2r}$ and $\phi_2(s) = \frac{p_x(s)-p_y-x(s)}{2r}$. We denote s_1, s_2, etc. the sequence of switching times along an extremal. During the first bang, since $\phi_1(0) = \frac{\alpha_1 r+p_y}{2r} > 0$ hence $u_1 = 1$, and since $\phi_2(0) = \frac{\alpha_1 r-p_y}{2r} \leq 0$ and $\dot{\phi}_2(0) = -\frac{u_1}{2}\lambda_z < 0$, the controls satisfy $u_1 = 1$ and $u_2 = -1$. Moreover

$$\begin{array}{lll} x(s) = 0, & p_x(s) = r\alpha_1 - rs, & \phi_1(s) = \frac{\alpha_1-s+1}{2}, \\ y(s) = rs, & p_y(s) = p_y(0) = r, & \phi_2(s) = \frac{\alpha_1-s-1}{2}. \\ z(s) = 0, & & \end{array}$$

The first switching time s_1 corresponds to $\phi_1(s_1) = 0$ hence $s_1 = 1 + \alpha_1$.

During the second bang, the controls satisfy $u_1 = -1$ and $u_2 = -1$ and

$$\begin{array}{lll} x(s) = -sr + r + \alpha_1 r, & p_x(s) = -r, & \phi_1(s) = \frac{-s+1+\alpha_1}{2}, \\ y(s) = r + \alpha_1 r, & p_y(s) = p_y(0) = r, & \phi_2(s) = \frac{s-3-\alpha_1}{2}. \\ z(s) = 0, & & \end{array}$$

The second switching time s_2 corresponds to $\phi_2(s_2) = 0$ hence $s_2 = 3 + \alpha_1$.

Along the third bang, the controls satisfy $u_1 = -1$ and $u_2 = 1$ and

$$\begin{array}{lll} x(s) = -2r, & p_x(s) = -\alpha_1 r - 4r + sr, & \phi_1(s) = \frac{-\alpha_1-5+s}{2}, \\ y(s) = 4r + 2\alpha_1 r - sr, & p_y(s) = p_y(0) = r, & \phi_2(s) = \frac{-\alpha_1-3+s}{2}. \\ z(s) = 2r(s - (3 + \alpha_1)), & & \end{array}$$

The third switching time s_3 corresponds to $\phi_1(s_3) = 0$ hence $s_3 = 5 + \alpha_1$.

During the fourth bang, the controls satisfy $u_1 = 1$ and $u_2 = 1$ and

$$\begin{array}{lll} x(s) = -7r - \alpha_1 r + sr, & p_x(s) = r, & \phi_1(s) = \frac{-5-\alpha_1+s}{2}, \\ y(s) = -r + \alpha_1 r, & p_y(s) = p_y(0) = r, & \phi_2(s) = \frac{7+\alpha_1-s}{2}. \\ z(s) = 4r^2, & & \end{array}$$

The fourth switching time s_4 corresponds to $\phi_2(s_4) = 0$ hence $s_4 = 7 + \alpha_1$.

Along the fifth bang, the controls satisfy $u_1 = 1$ and $u_2 = -1$ and

$$\begin{array}{lll} x(s) = 0, & p_x(s) = 8r + \alpha_1 r - sr, & \phi_1(s) = \frac{9+\alpha_1-s}{2}, \\ y(s) = -r + \alpha_1 r + sr, & p_y(s) = p_y(0) = r, & \phi_2(s) = \frac{7+\alpha_1-s}{2}. \\ z(s) = 4r^2, & & \end{array}$$

The fifth switching time s_5 corresponds to $\phi_1(s_5) = 0$ hence $s_5 = 9 + \alpha_1$.

The other extremals with $\lambda_z \neq 0$ can be computed the same way and are very similar. Finally, extremals with $\lambda_z > 0$ have projections in the (x, y)-plane which are squares and the z-coordinate after one turn of the square is equal to the area of the square. This implies that they are all optimal until the end of this turn that is until $s = 8$ or $t = \frac{8}{p_z}$. After they lose optimality, crossing one each other transversaly. As a consequence the cut time is $s = 8$ or $t = 8r$ and the cut locus is the vertical axis (as in the Heisenberg case in sub-riemannian geometry).

4.2 Extremal with $\lambda_z = 0$

What about the extremals with $\lambda_z = 0$? For such an extremal, λ is constant and $\phi_1 = \frac{\lambda_x+\lambda_y}{2}$ and $\phi_2 = \frac{\lambda_x-\lambda_y}{2}$ are also constant. If both are not zero hence u_1 and u_2 are constants along the extremal, the corresponding curve is optimal and is an extremal. If $\phi_1 \equiv 0$ and $\phi_2 \equiv 1$ then the extremal is u_1-singular and the control u_1 is not determined by the max condition of the PMP. In fact in this case, one proves easily that for any choice of $u_1(.)$ such that $|u_1(t)| \leq 1$, one gets for any $T > 0$, a minimizer from $(0, 0, 0)$ to $(\frac{\int_0^T u_1(t)dt+T}{2}, \frac{\int_0^T u_1(t)dt-T}{2}, z)$ where

$$z = \int_0^T \frac{(u_1(t) - 1)(\int_0^t u_1(\tau)d\tau + t)}{4} dt.$$

The proof comes from the fact that the projection of this point on the (x, y)-plane is on the segment between the two points (T, 0) and (0, -T). The same kind of computation can be done for $\phi_1 \equiv 0$ and $\phi_2 \equiv -1$ or $\phi_1 \equiv \pm 1$ and $\phi_2 \equiv 0$.

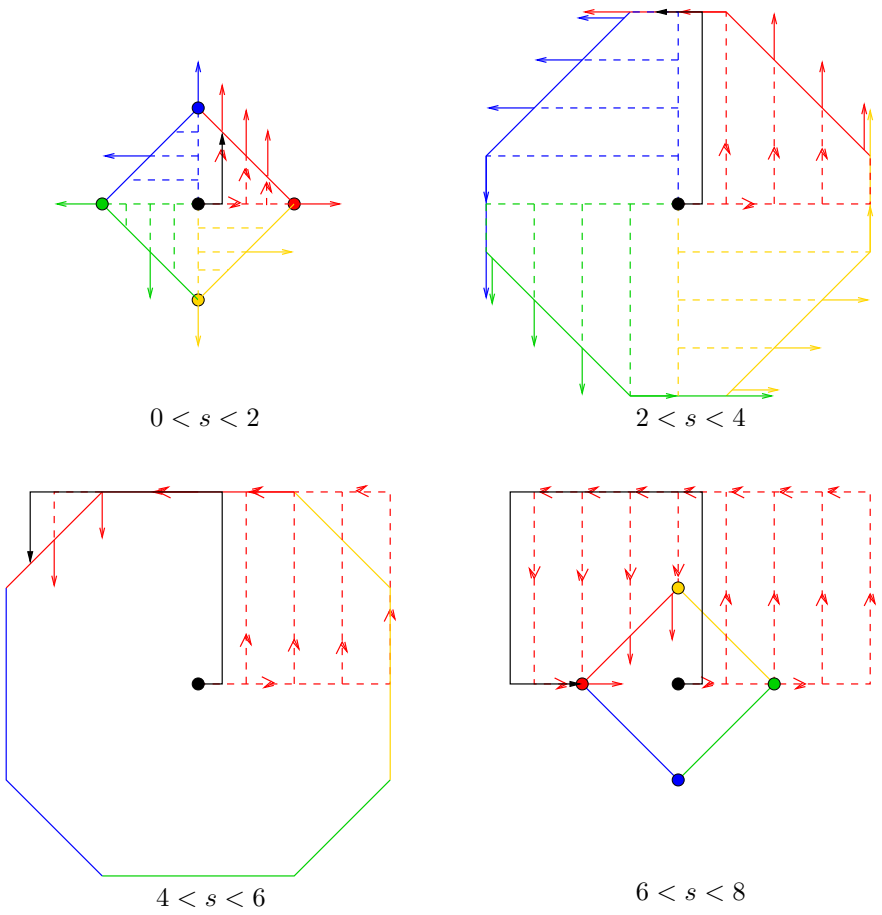

Figure 1: Evolution of the front at $r \neq 0$ fixed. In red dot lines and in black the extremals with initial speed G_1, in full line the front at 4 different times, with four colors corresponding to the four possible initial speeds

4.3 Exponential map

Let us concentrate again on the extremals with $\lambda_z \neq 0$. One can consider the *exponential map* which to (r, α, s) where $\alpha \in [-1, 1[$, $r > 0$, $s \geq 0$ associates the end point of the extremal with initial condition $\lambda_x = \alpha$, $\lambda_y = 1$ and $\lambda_z = \frac{1}{r}$ for the time $t = rs$. This map is smooth at points with $-1 < \alpha < 1$, $s_i(p_x, r) < s < s_{i+1}(p_x, r)$ for a certain i where $s_j(p_x, r)$ is the j^{th} switching time of the extremal with initial condition p_x, $p_y = 1$ and r. The same can be done for $\lambda_y = -1$ or $\lambda_x = \pm 1$ and $\lambda_y \in [-1, 1]$. Since it is smooth for $-r < p_x < r$ and $s \neq s_i$ $\forall i$, we can compute its jacobian. It happens that it is null during the two first bangs, and that it has opposite sign to the one of r during the third and fourth bangs. It is again null during the fifth bang. As we will see later for r small in the generic cases, the jacobian will not be null during the third and fourth bangs also. In the nilpotent case, the first conjugate time is $t_5 = rs_5$ and for $t \in]rs_4, rs_5[$, $Jac(t) = 0$.

4.4 Geometric objects

Since the conjugate time is t_5, the first conjugate locus is the set of points where an extremal switches for the fifth time. The first conjugate locus is

$$\{(2\delta r, 0, \pm 4r^2) | r \in \mathbb{R}, \delta \in]-1, 1[\} \cup \{(0, 2\delta r, \pm 4r^2) | r \in \mathbb{R}, \delta \in]-1, 1[\}.$$

The Maxwell set is exactly the same set.

Figure 2 shows the conjugate locus and three points of view of the part of the sphere that is reached by non singular extremals.

5 Extremals with both controls switching

In this section, we present the computation of jets of extremals with large covector $|\lambda|$ and of geometric objects attached to them: switching locus and conjugate locus. As in the nilpotent case, we can define a Hamiltonian flow which, to an initial condition $(\lambda_x, \lambda_y, \lambda_z)$ (with $\max(|\lambda_x|, \lambda_y|) = 1$) associates the end point at time t of the solution of the dynamics

$$\begin{aligned}
\dot{x} &= \frac{u_1 + u_2}{2} + \frac{u_1 - u_2}{2}(a_{200}x^2 + a_{110}xy + \theta_x), \\
\dot{y} &= \frac{u_1 - u_2}{2}(1 + b_{200}x^2 + b_{110}xy + \theta_y), \\
\dot{z} &= \frac{u_1 - u_2}{2}(x + c_{200}x^2 + c_{110}xy + c_{300}x^3 + c_{210}x^2y + c_{120}y^2x + \theta_z), \\
\dot{\lambda_x} &= -\frac{u_1 - u_2}{2}(\lambda_x(2a_{200}x + a_{110}y) + \lambda_y(2b_{200}x + b_{110}y) \\
&\quad + \lambda_z(1 + 2c_{200}x + 3c_{300}x^2 + c_{110}y + 2c_{210}xy + c_{120}y^2)), \\
\dot{\lambda_y} &= -\frac{u_1 - u_2}{2}(a_{110}x\lambda_x + b_{110}x\lambda_y + \lambda_z(c_{110}x + c_{210}x^2 + 2c_{120}xy)), \\
\dot{\lambda_z} &= \frac{u_1 - u_2}{2}\lambda_z x(c_{201}x + c_{111}y),
\end{aligned}$$

$$\begin{aligned}
u_1(t) = sign(\phi_1(t)), \quad u_2(t) = sign(\phi_2(t)), \\
\phi_1(t) = \lambda(t)F_1(q(t)), \quad \phi_2(t) = \lambda(t)F_2(q(t)).
\end{aligned}$$

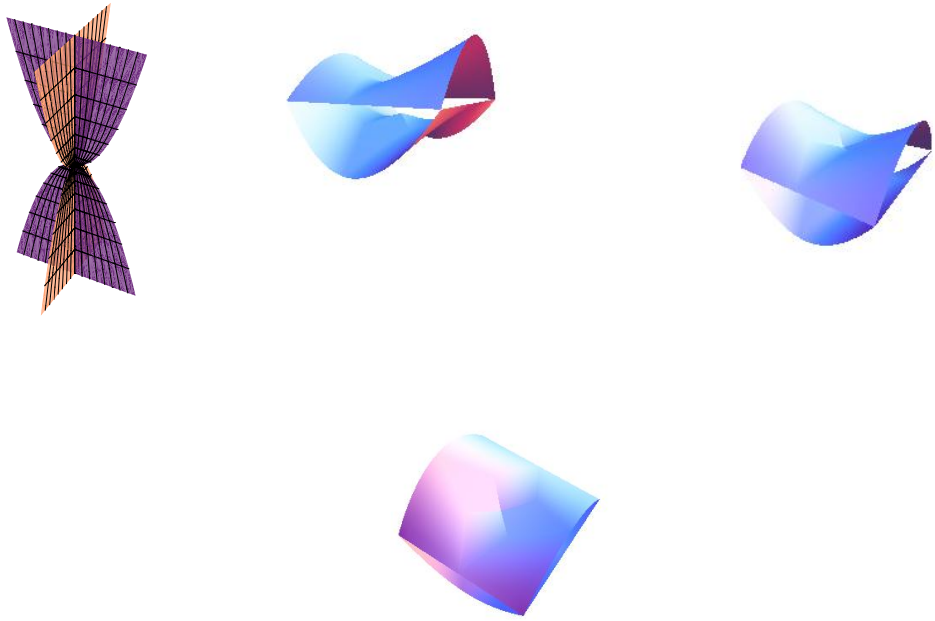

Figure 2: The conjugate locus and three points of view of the non singular part of the sphere in the nilpotent case

From now $\dot{x}$ denotes $\frac{dx}{ds}$. Using the change of coordinates for (x, y, z, p, r, s). we can define a new Hamiltonian flow by the dynamics

$$\begin{aligned}
\dot{x} &= \frac{u_1+u_2}{2}r + \frac{u_1+u_2}{2}r(a_{200}x^2 + a_{110}xy + \theta_x),\\
\dot{y} &= \frac{u_1-u_2}{2}r(1 + b_{200}x^2 + b_{110}xy + \theta_y),\\
\dot{z} &= \frac{1}{2}r(\theta_z(u_1+u_2) + (u_1-u_2)(x + c_{200}x^2 + c_{300}x^3 + c_{110}xy + c_{210}x^2y + c_{120}xy^2)),\\
\dot{p}_x &= -\frac{u_1-u_2}{2}r(1 + 2c_{200}x + p_x(2a_{200}x + a_{110}y) + p_y(2b_{200}x + b_{110}y) + 3c_{300}x^2\\
&\quad + c_{110}y + 2c_{210}xy + c_{120}y^2),\\
\dot{p}_y &= -\frac{u_1-u_2}{2}r(c_{110}x + a_{110}p_x x + b_{110}p_y x + c_{210}x^2 + 2c_{120}xy),\\
\dot{r} &= \frac{u_1-u_2}{2}r^2 x(c_{201}x + c_{111}y).
\end{aligned}$$

$$\begin{aligned}
\phi_1(t) &= \tfrac{1}{r}pF_1(q(t)), \qquad \phi_2(t) = \tfrac{1}{r}pF_2(q(t))\\
u_1(t) &= sign(\phi_1(t)), \qquad u_2(t) = sign(\phi_2(t)).
\end{aligned}$$

Since the set of initial condition is a square for (p_x, p_y), we define in fact four Hamiltonian flows for each initial speed $(G_1, -G_1, G_2, -G_2)$. For example, for the extremals with initial speed equal to G_2 we have $p_y(0) = r$ and $p_x = \alpha r$ with $\alpha \in]-1, 1]$. The new Hamiltonian flow as for variables (r_0, α, s) where $r_0 = r(0)$, $p_x(0) = \alpha r$ and $s = \frac{t}{r_0}$. In order to compute jets of the Hamiltonian flow we write

$$\begin{aligned}
x(r_0,\alpha,s) &= x_1(\alpha,s)r_0 + x_2(\alpha,s)r_0^2 + x_3(\alpha,s)r_0^3 + X_4(r_0,\alpha,s)r_0^4,\\
y(r_0,\alpha,s) &= y_1(\alpha,s)r_0 + y_2(\alpha,s)r_0^2 + y_3(\alpha,s)r_0^3 + Y_4(r_0,\alpha,s)r_0^4,\\
z(r_0,\alpha,s) &= z_2(\alpha,s)r_0^2 + z_3(\alpha,s)r_0^3 + z_4(\alpha,s)r_0^4 + Z_5(r_0,\alpha,s)r_0^5,\\
p_x(r_0,\alpha,s) &= p_{x1}(\alpha,s)r_0 + p_{x2}(\alpha,s)r_0^2 + p_{x3}(\alpha,s)r_0^3 + P_{x4}(r_0,\alpha,s)r_0^4,\\
p_y(r_0,\alpha,s) &= p_{y1}(\alpha,s)r_0 + p_{y2}(\alpha,s)r_0^2 + p_{y3}(\alpha,s)r_0^3 + P_{y4}(r_0,\alpha,s)r_0^4,\\
r(r_0,\alpha,s) &= r_0 + r_2(\alpha,s)r_0^2 + r_3(\alpha,s)r_0^3 + R_4(r_0,\alpha,s)r_0^4.
\end{aligned}$$

where all the new functions are smooth functions of their variables. Using this dynamics we find the following. For the first order

$$\begin{array}{ll}
\dot{x}_1 = \frac{u_1+u_2}{2}, & \dot{p}_{x1} = \frac{-u_1+u_2}{2},\\
\dot{y}_1 = \frac{u_1-u_2}{2}, & \dot{p}_{y1} = 0,\\
\dot{z}_2 = \frac{u_1-u_2}{2}x_1. &
\end{array}$$

For the second order

$$\begin{array}{ll}
\dot{x}_2 = 0, & \dot{p}_{x2} = -\frac{u_1-u_2}{2}(2c_{200}x_1 + c_{110}y_1),\\
\dot{y}_2 = 0, & \dot{p}_{y2} = -\frac{u_1-u_2}{2}c_{110}x_1,\\
\dot{z}_3 = \frac{u_1-u_2}{2}(x_2 + x_1(c_{200}x_1 + c_{110}y_1)), & \dot{r}_2 = 0.
\end{array}$$

For the third order

$$\begin{aligned}
\dot{x}_3 &= \frac{u_1-u_2}{2}(a_{200}x_1^2 + a_{110}x_1y_1),\\
\dot{y}_3 &= \frac{u_1-u_2}{2}(b_{200}x_1^2 + b_{110}x_1y_1),\\
\dot{z}_4 &= \frac{u_1-u_2}{2}(c_{300}x_1^3 + 2c_{200}x_1x_2 + x_3 + c_{110}x_2y_1 + c_{110}x_1y_2 + c_{210}x_1^2y_1 + c_{120}x_1y_1^2),\\
\dot{p}_{x3} &= -\frac{u_1-u_2}{2}(2a_{200}p_{x_1}x_1 + 2b_{200}p_{y_1}x_1 + 2c_{200}x_2 + 3c_{300}x_1^2\\
&\quad + a_{110}p_{x_1}y_1 + b_{110}p_{y_1}y_1 + c_{110}y_2 + 2c_{210}x_1y_1 + c_{120}y_1^2),\\
\dot{p}_{y3} &= \frac{u_1-u_2}{2}(-c_{110}x_2 - x_1(a_{110}p_{x_1} + b_{110}p_{y_1} + c_{210}x_1 + 2c_{120}y_1)),\\
\dot{r}_3 &= 0.
\end{aligned}$$

Recall that the extremals we are interested in have initial condition

$$\begin{array}{ll}
x(r_0,\alpha,0) = 0, & p_x(r_0,\alpha,0) = r_0p_{x1}(\alpha,0),\\
y(r_0,\alpha,0) = 0, & p_y(r_0,\alpha,0) = r_0p_{y1}(\alpha,0),\\
z(r_0,\alpha,0) = 0, & r(r_0,\alpha,0) = r_0.
\end{array}$$

These equations are integrable hence we can compute jets of switching functions and hence jets of switching times. Finally, we are able to compute the jets of the different bangs of the extremals.

If we restrict the computation to x, y, z as functions of (r_0, α, s) for the four Hamiltonian flows, we get four exponential maps that we denote Exp_β where $\beta = -1, 1, -2$ or 2 depending on if the initial velocity is $-G_1$, G_1, $-G_2$, G_2.

It happens that all the extremals computed that way are turning extremals like in 3D contact sub-riemannian geometry. For example, if $r_0 > 0$ and if the extremal starts with G_1 then after it switches to G_2, then $-G_1$, $-G_2$, G_1 and so on.

In [29], M. Sigalotti proves, studying second order optimality conditions, that this familly of extremals cannot be optimal after the fifth switch.

For these exponential maps, one can compute their jacobian for each bang arc. One finds

- $Jac(\mathrm{Exp}_{\pm 2}) = 0$ for $0 < s < s_2, s \neq s_1$,
- $Jac(\mathrm{Exp}_{\pm 2}) = -8r_0^3 + o(r_0^3)$ for $s_2 < s < s_3$,
- $Jac(\mathrm{Exp}_{\pm 2}) = -8r_0^3 + o(r_0^3)$ for $s_3 < s < s_4$,
- $Jac(\mathrm{Exp}_{\pm 2}) = 32(2c_{120} - c_{110}^2)r_0^5 + o(r_0^5)$ for $s_4 < s < s_5$,
- $Jac(\mathrm{Exp}_{\pm 2}) = 8r_0^3 + o(r_0^3)$ for $s_5 < s < s_6$,

and

- $Jac(\mathrm{Exp}_{\pm 1}) = 0$ if $0 < s < s_1$ or $s_1 < s < s_2$,
- $Jac(\mathrm{Exp}_{\pm 1}) = -4r_0^3 + o(r_0^3)$ if $s_2 < s < s_3$,
- $Jac(\mathrm{Exp}_{\pm 1}) = -8r_0^3 + o(r_0^3)$ if $s_3 < s < s_4$,
- $Jac(\mathrm{Exp}_{\pm 1}) = 64(3c_{300} - 2b_{200} - 2c_{200}^2)r_0^5 + o(r_0^5)$ if $s_4 < s < s_5$,
- $Jac(\mathrm{Exp}_{\pm 1}) = 8r_0^3 + o(r_0^3)$ if $s_5 < s < s_6$.

We can now state the following proposition which shows that the sign of the Jacobian is an important invariant which determines the conjugate time.

Proposition 12. *Let G_1 and G_2 as in the normal form given in section 2.*

- *If $C_1 = 3c_{300} - 2b_{200} - 2c_{200}^2 > 0$ then the fourth switching time t_4 is the first conjugate time for extremal with initial velocity $\pm G_1$. If $C_1 < 0$ then it is the fifth t_5.*
- *If $C_2 = 2c_{120} - c_{110}^2 > 0$ then the fourth switching time t_4 is the first conjugate time for extremals with initial velocity $\pm G_2$. If $C_2 < 0$ then it is the fifth t_5.*

Still using the expressions given in Appendix, we can give the expressions of the upper part of the first conjugate locus for the four exponential maps.

For $Exp_{\pm 1}$, if $C_1 > 0$

$$\begin{aligned} x_{conj} &= \pm(\alpha_2 - 1)r_0 + (4c_{110} - c_{200}(\alpha_2 - 1)^2)r_0^2 + o(r_0^2), \\ y_{conj} &= -8c_{200}r_0^2 \pm 4(b_{110} + 6c_{110}c_{200} - 2c_{210} \\ &\qquad + (4b_{200} + 12c_{200}^2 - 6c_{300})\alpha_2)r_0^3 + o(r_0^3), \\ z_{conj} &= 4r_0^2 \mp 8(c_{110} + 2c_{200}\alpha_2)r_0^3 + o(r_0^3), \end{aligned}$$

and if $C_1 < 0$

$$\begin{aligned} x_{conj} &= \pm(1+\alpha_2)r_0 + (4c_{110} - c_{200}(1+\alpha_2)^2)r_0^2 + o(r_0^2), \\ y_{conj} &= -8c_{200}r_0^2 \pm 4(b_{110} + 6c_{110}c_{200} - 2c_{210} \\ &\qquad +(4b_{200} + 12c_{200}^2 - 6c_{300})\alpha_2)r_0^3 + o(r_0^3), \\ z_{conj} &= 4r_0^2 \mp 8(c_{110} + 2c_{200}\alpha_2)r_0^3 + o(r_0^3), \end{aligned}$$

and for $Exp_{\pm 2}$, if $C_2 > 0$

$$\begin{aligned} x_{conj} &= 4c_{110}r_0^2 \pm 4(b_{110} + 6c_{110}c_{200} - 2c_{210} \\ &\qquad +\alpha_1(2c_{120} - 3c_{110}^2))r_0^3 + o(r_0^3), \\ y_{conj} &= \pm(-1+\alpha_1)r_0 - \frac{1}{2}(16c_{200} + c_{110}(\alpha_1 - 1)^2)r_0^2 + o(r_0^2), \\ z_{conj} &= 4r_0^2 \pm 4(4c_{200} - c_{110}(1+\alpha_1))r_0^3 + o(r_0^3), \end{aligned}$$

and if $C_2 < 0$

$$\begin{aligned} x_{conj} &= 4c_{110}r_0^2 \pm 4(b_{110} + 6c_{110}c_{200} - 2c_{210} \\ &\qquad +\alpha_1(2c_{120} - 3c_{110}^2))r_0^3 + o(r_0^3), \\ y_{conj} &= \pm(1+\alpha_1)r_0 - \frac{1}{2}(16c_{200} + c_{110}(1+\alpha_1)^2)r_0^2 + o(r_0^2), \\ z_{conj} &= 4r_0^2 \pm 4(4c_{200} + c_{110}(1-\alpha_1))r_0^3 + o(r_0^3). \end{aligned}$$

6 Local Cut Locus of extremals with $\lambda_z(0) >> 1$

In the nilpotent case, the extremals with $|\alpha| < 1$ reach the Maxwell set at the fourth switch when, for those with $|\alpha| = 1$, it is at the third switch. When $C_1 \neq 0$ and $C_2 \neq 0$ we will see that the cut is reached during the fourth or fifth bang.

From section 4, we can conclude that the loss of optimality may come during the fourth bang or the fifth bang. Moreover, in [29] the author proves that the extremals we are considering cannot be optimal after the fifth switch. Hence we can conclude that the cut locus comes from the intersection of two fourth bangs of different exp_i, the intersection of two fifth bangs of different exp_i, the intersection of a fourth bang and a fifth bang of two different exp_i.

In the following we compute, for the jets of order 3, 3 and 4 of x, y and z in r_0, the possible intersections listed previously, and finally describe the possible pictures of the cut locus depending on the values of invariants of the structure appearing in the normal form. Finally we discuss the stability of the pictures.

6.1 Intersections of fourth bangs

6.1.1 Intersection of an extremal starting with $\pm G_1$ with one starting with $\pm G_2$

As seen in the nilpotent case, an extremal starting with $\pm G_1$ and $|\alpha_2| < 1$ meets the Maxwell set at $s = s_4$ and intersect at this time the extremal starting with $\pm G_2$ and $\alpha_1 = 1$. Hence, we compute the jets of $Exp_{\pm 1}$ close to the fourth switch time that is at $s = 7 + \alpha_2 + T_2 r_0 + T_3 r_0^2$ and the jets

of $Exp_{\pm 2}$ for $r_0' = r_0 + R_2 r_0^2 + R_3 r_0^3$, $\alpha_1 = 1 - \alpha_{11} r_0 - \alpha_{12} r_0^2$ and at time $s' = s\frac{r_0}{r_0'}$. Asking that the corresponding points are the same, one gets

$$\begin{aligned} R_2 &= \mp 2c_{200}(1+\alpha_2) \\ T_2 &= \mp 8c_{110} - c_{200}(1 + 14\alpha_2 + \alpha_2^2) \\ \alpha_{11} &= 0 \end{aligned}$$

and

$$\begin{aligned} R_3 &= \frac{(1+\alpha_2)}{2}(3b_{110} + 6c_{110}c_{200} + 4c_{200}^2(1+3\alpha_2) \\ &\qquad +4b_{200}(-1+\alpha_2) + 6c_{300}(1-\alpha_2) - 6c_{210}) \\ T_3 &= \frac{16}{3}a_{110} + 20c_{110}^2 - a_{200} + 8b_{200} + 38c_{200}^2 - \frac{40}{3}c_{120} - 27c_{300} \\ &\quad +(8b_{110} + 2a_{200} + 9b_{200} + 48c_{110}c_{200} + 14c_{200}^2 - 15c_{300} - 16c_{210})\alpha_2 \\ &\quad +(-a_{200} + 14b_{200} + 42c_{200}^2 - 21c_{300})\alpha_2^2 \\ &\quad +(b_{200} + 2c_{200}^2 - c_{300})\alpha_2^3 \\ \alpha_{12} &= 4(1+\alpha_2)(3c_{300} - 2b_{200} - 2c_{200}^2) = 4(1+\alpha_2)C_1 \end{aligned}$$

We see here that in order the intersection exists, $\alpha_1 = 1 - \alpha_{11} r_0 - \alpha_{12} r_0^2$ should be less or equal to 1 hence, since $\alpha_{11} = 0$, one should have $\alpha_{12} > 0$ which implies $C_1 > 0$.

When $C_1 > 0$, once computed the corresponding points (depending on r_0 and α_2) one can compute the suspension of this part of the cut locus by looking at its intersection with $z = 4\rho^2$ for ρ small. One gets

$$\begin{aligned} x_{cut} &= \pm(-1+\alpha_2)\rho + (3c_{110} - c_{200} + c_{110}\alpha_2 + c_{200}\alpha_2^2)\rho^2 \\ &\quad \pm\frac{1}{2}(a_{110} - 7c_{110}^2 - 2a_{200} + 2b_{200} - 8c_{110}c_{200} + 4c_{200}^2 + 12c_{120} - 4c_{300} \\ &\quad +(4a_{200} - a_{110} - 5b_{110} - c_{110}^2 - 6c_{110}c_{200} - 4c_{200}^2 + 4c_{120} + 10c_{210})\alpha_2 \\ &\quad +(6c_{210} - 3b_{110} - 2a_{200} - 2c_{110}c_{200})\alpha_2^2 + (4c_{300} - 2b_{200})\alpha_2^3)\rho^3 \\ y_{cut} &= -8c_{200}\rho^2 \pm (4b_{110} + 8c_{110}c_{200} + (8b_{200} - 12c_{300} + 8c_{200}^2)(\alpha_2 - 1))\rho^3 \\ z_{cut} &= 4\rho^2 \end{aligned}$$

6.1.2 Intersection of an extremal starting with $\pm G_2$ with one starting with $\mp G_1$

The same computations can be done for extremals starting by $\pm G_2$ and intersecting $\mp G_1$ and one gets that C_2 should be positive. Hence

$$\begin{aligned}
x_{cut} &= 4c_{110}\rho^2 \pm (4b_{110} + 8c_{110}c_{200} - 8c_{210} + (6c_{110}^2 - 4c_{120})(1-\alpha_1))\rho^3 \\
y_{cut} &= \pm(-1+\alpha_1)\rho + (-c_{110} - 6c_{200} + c_{110}\alpha_1 - 2c_{200}\alpha_1)\rho^2 \\
&\quad \pm\frac{1}{24}(4a_{110} - 24b_{110} - 21c_{110}^2 - 312b_{200} - 144c_{110}c_{200} - 336c_{200}^2 \\
&\quad -4c_{120} + 432c_{300} + 24c_{210} + (108b_{110} + 51c_{110}^2 - 72b_{200} \\
&\quad +264c_{110}c_{200} - 48c_{200}^2 - 36c_{120} + 144c_{300} - 168c_{210})\alpha_1 \\
&\quad +12(b_{110} - 27c_{110}^2 + 72c_{110}c_{200} + 36c_{120} - 48c_{210})\alpha_1^2 \\
&\quad +(4c_{120} - 4a_{110} - 3c_{110}^2)\alpha_1^3)\rho^3 \\
z_{cut} &= 4\rho^2
\end{aligned}$$

6.1.3 Intersection of the front starting with G_1 with the one starting with $-G_1$

Such a self-intersection of the front can take place only at $s = 8 + O(r_0)$ as in the nilpotent case. In order to compute such intersection close to $s = 8$, we proceed as follows. We compute the intersection of these parts of the front with $z = 4\rho^2$ for ρ^2. In order to do this, we fix $t = 8\rho + T_2\rho^2 + T_3\rho^3$, for each type of extremal fix $\alpha_2 = 1 - \alpha_{21}\rho - \alpha_{22}\rho^2$ and find the r_0 such that the corresponding point $Exp_{\pm 1}(r_0, \alpha, t/r_0)$ satisfies $z = 4\rho^2$. For the extremals starting by $\pm G_1$ one finds

$$\begin{aligned}
x_{sus} &= (4c_{110} \mp \alpha_{21})\rho^2 \mp (+4b_{110} + 4c_{110}^2 \pm 4c_{200}\alpha_{21} \\
&\qquad +2c_{110}(4c_{200} \pm \alpha_{21}) + \alpha_{22} - 8c_{120} - 8c_{210})\rho^3 \\
y_{sus} &= (-8c_{200} \mp \alpha_{21} \mp T_2)\rho^2 \pm (\frac{4}{3}a_{110} - \alpha_{21}^2 - \alpha_{22} + 8b_{200} \pm 2\alpha_{21}c_{110} \\
&\quad +\frac{8}{3}c_{120} \mp 4\alpha_{21}c_{200} + 16c_{110}c_{200} + 16c_{200}^2 - 16c_{300} - \alpha_{21}T_2 \pm 4c_{110}T_2 - T_3)\rho^3 \\
z_{sus} &= 4\rho^2
\end{aligned}$$

It is then easy to show that, in order to get a contact between these two fronts, T_2 should be equal to 0 and $\alpha_{21+} = -\alpha_{21-}$. But, since both should be positive hence $\alpha_{21+} = \alpha_{21-} = 0$ and this implies that T_3 should be equal to

$$T_{3b} = \frac{4}{3}(a_{110} + 3b_{110} + 6b_{200} + 3c_{110}^2 - 4c_{120} + 18c_{110}c_{200} + 12c_{200}^2 - 6c_{210} - 12c_{300}).$$

At this time, with $\alpha_{21+} = \alpha_{21-} = 0$, the two fronts are segments belonging to the same line.

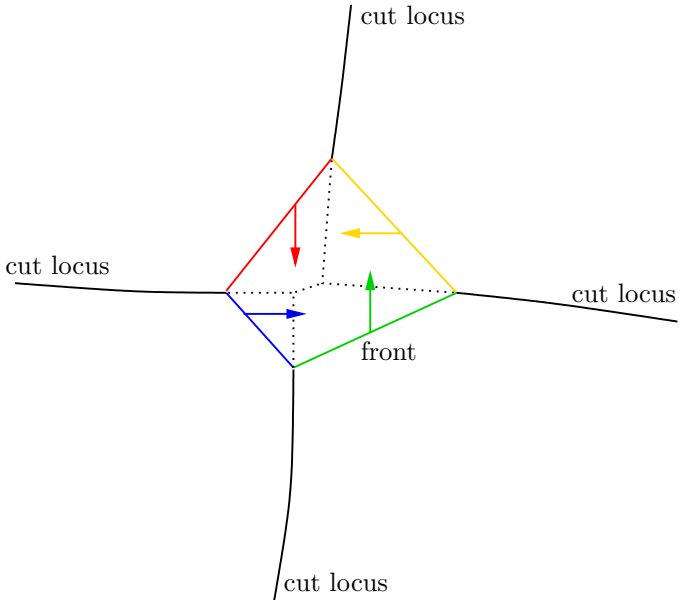

Figure 3: Closure of the cut locus at z fixed.

6.1.4 Intersection of the front starting with G_2 with the one starting with $-G_2$

We proceed the same way. For the extremals starting by $\pm G_2$ one finds

$$\begin{aligned} x_{sus} &= (4c_{110} \pm \alpha_{11} \pm T_2)\rho^2 \pm (-\frac{4}{3}a_{110} - 4c_{110}^2 + 8b_{200} \mp 4c_{200}\alpha_{11} \\ &\quad -2c_{110}(8c_{200} \pm \alpha_{11}) + \alpha_{12} + \frac{16}{3}c_{120} - 8c_{300} + T_3)\rho^3 \\ y_{sus} &= -(8c_{200} \pm \alpha_{11})\rho^2 \pm (4b_{110} - 16b_{200} + 8c_{110}c_{200} - 16c_{200}^2 \\ &\quad \mp 2c_{110}\alpha_{11} \pm 4c_{200}\alpha_{11} - \alpha_{12} + 24c_{300} - 8c_{210})\rho^3 \\ z_{sus} &= 4\rho^2 \end{aligned}$$

It is then easy to show that, in order to get a contact between these two fronts, T_2 should be equal to 0 and $\alpha_{11+} = -\alpha_{11-}$. But, since both should be positive hence $\alpha_{11+} = \alpha_{11-} = 0$ and this implies that T_3 should be equal to

$$T_{3a} = \frac{4}{3}(a_{110} - 3b_{110} + 6b_{200} + 3c_{110}^2 - 4c_{120} + 6c_{110}c_{200} + 12c_{200}^2 + 6c_{210} - 12c_{300}).$$

6.2 Cut locus when $C_1 > 0$ and $C_2 > 0$

With the considerations given before, if $C_1 > 0$, $C_2 > 0$ and $T_{3a} \neq T_{3b}$, the intersection of the cut locus with $\{z = 4\rho^2\}$ is constituted of 5 branches as in the Figure 3.

The four external branches comes from the intersection of the fourth bangs of $\exp_{\pm 1}$ with $\exp_{\pm 2}$ and of the fourth bangs of $\exp_{\pm 1}$ with $\exp_{\mp 2}$, see Figure 3. The central branch is the intersection

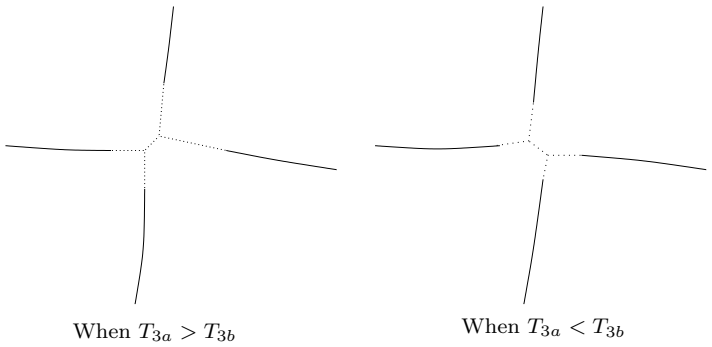

Figure 4: Closure of the cut locus at z fixed

of the fourth bangs of $\exp_1$ with $\exp_{-1}$ if $T_{3b} < T_{3a}$ or of the fourth bangs of $\exp_2$ with $\exp_{-2}$ if $T_{3a} < T_{3b}$, see Figure 4.

After $\min\{T_{3a}, T_{3b}\}$ all the extremals participating to the construction of this part of the cut locus have lost optimality.

Finally the picture of the cut depends on the sign of

$$T_{3a} - T_{3b} = -8(b_{110} + 2c_{110}c_{200} - 2c_{210}).$$

If $T_{3a} > T_{3b}$ then the two points of the cut locus that connect three branches are with

$$\begin{aligned} x &= 4c_{110}\rho^2 \pm C\rho^3 + o(\rho^3) \\ y &= -8c_{200}\rho^2 \pm C\rho^3 + o(\rho^3) \\ z &= 4\rho^2 \end{aligned}$$

with $C = 4(b_{110} + 2c_{110}c_{200} - 2c_{210})$, when if $T_{3a} < T_{3b}$ then the two points of the cut locus that connect three branches satisfy

$$\begin{aligned} x &= 4c_{110}\rho^2 \pm C\rho^3 + o(\rho^3) \\ y &= -8c_{200}\rho^2 \mp C\rho^3 + o(\rho^3) \\ z &= 4\rho^2 \end{aligned}$$

Finally we can present the upper part of the cut locus when $C_1 > 0$ and $C_2 > 0$ in Figure 5

6.3 Suspension of fifth bang front

At $6 < s < 8$, the part of the front corresponding to the fifth bang is close to $(\pm(s-8)\rho, 0, 4\rho^2)$ for the front starting with $\pm G_1$ and close to $(0, \pm(s-8)\rho, 4\rho^2)$ for the front starting with $\pm G_2$. Hence the intersections come at s close to 8.

In order to compute these intersections we fix a small ρ, consider a time $t = 8\rho + T_2\rho^2 + T_3\rho^3$, and for each type of extremal find the r_0 such that the corresponding point $Exp_{\pm 1}(r_0, \alpha, t/r_0)$

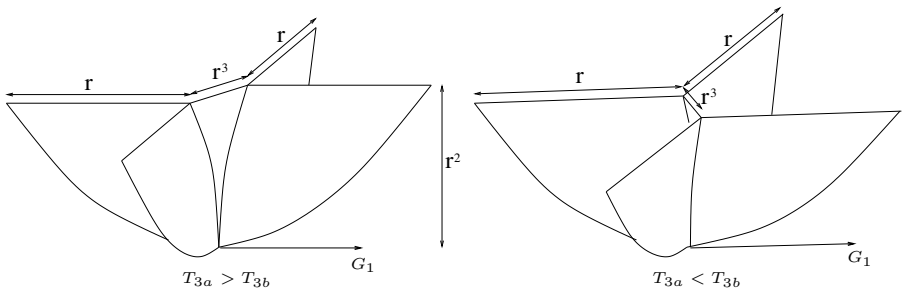

Figure 5: The upper part of the cut locus

satisfies $z = 4\rho^2$. For the extremals starting by $\pm G_1$ one finds $exp_{\pm 1}$

$$\begin{aligned} x_{\pm 1sus} &= (4c_{110} \pm T_2)\rho^2 \pm (\frac{16}{3}c_{120} - \frac{4}{3}a_{110} - 4c_{110}^2 - 16c_{110}c_{200} - 8c_{200}^2 \\ &\quad +4c_{300} + T_3 - 4C_1\alpha_2^2)\rho^3 \\ y_{\pm 1sus} &= -8c_{200}\rho^2 \pm (4b_{110} + 8c_{110}c_{200} - 8c_{210} - 8C_1\alpha_2)\rho^3 \\ z_{\pm 1sus} &= 4\rho^2 \end{aligned}$$

For the extremals starting by $\pm G_2$ one finds $exp_{\pm 2}$

$$\begin{aligned} x_{\pm 2sus} &= 4c_{110}\rho^2 \pm (4b_{110} + 8c_{110}c_{200} - 8c_{210} + 4C_2\alpha_1)\rho^3 \\ y_{\pm 2sus} &= (-8c_{200} \pm T_2)\rho^2 \pm (\frac{4}{3}c_{120} - \frac{4}{3}a_{110} - 8b_{200} - 16c_{200}^2 - 2c_{110}^2 \\ &\quad +16c_{300} + 4c_{110}(-4c_{200} \pm T_2) + T_3 - 2C_2\alpha_1^2)\rho^3 \\ z_{\pm 2sus} &= 4\rho^2 \end{aligned}$$

As one can see, the intersection of the fifth bang front at t with the plane $z = 4\rho^2$ is the union of arc of parabolas. If we consider all these curves for $\alpha_i \in [0, 1]$ we can observe that the tangents at $\alpha = \pm 1$ are line with equations of the $x + y = c$ or $x - y = c$. Moreover, this tangent at $\alpha_2 = -1$ of the fifth bang front of $\exp_{\pm 1}$ is tangent to the fourth bang at the corresponding α_1 of $\exp_{\pm 2}$, and the tangent at $\alpha_1 = -1$ of the fifth bang front of $\exp_{\pm 2}$ is tangent to the fourth bang at the corresponding α_2 of $\exp_{\pm 1}$.

Moreover remark that, at $T_2 = 0$, the intersection of the front with $z = 4\rho^2$ still has a central symmetry at this order of jets, centred at

$$(x, y) = (4c_{110}\rho^2, -8c_{200}\rho^2).$$

6.4 Cut locus when $C_1 > 0$ and $C_2 < 0$

If $C_1 > 0$ and $C_2 < 0$ then the picture of the front at $t < 8\rho$ is as in the Figure 6. The fifth bang of $\exp_{\pm 1}$ do not participate to the optimal synthesis and the fourth bang front of $\exp_{\pm 1}$ intersect the fourth bang front of $\exp_{\pm 2}$. The fifth bang front of $\exp_{\pm 2}$ is optimal.

Let consider the closure of the cut, that it when $t = 8\rho + T_2\rho^2 + T_3\rho^3$. Wa can identify the following subcases

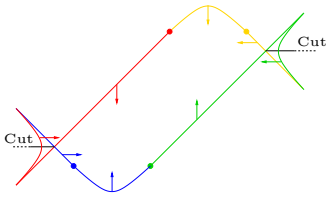

Figure 6: The front before $t = 8\rho$ when $C_1 > 0$ and $C_2 < 0$

- When $4b_{110} + 8c_{110}c_{200} - 8c_{210} - 4C_2 < 0$ then all the fifth bang of $\exp_2$ satisfies $x < 4c_{110}\rho^2$ when all the fifth bang of $\exp_{-2}$ satisfies $x > 4c_{110}\rho^2$. This implies that the sequel of the self intersections of the front is the following : first the fourth bang front of $\exp_{\pm 1}$ intersect the fourth bang front of $\exp_{\pm 2}$; then at time $T_2 = 0$, $T_3 = T_{3c} = T_{3b} + \frac{4}{3}C_2 - \frac{8}{3}c_{110}^2 < T_{3b}$ the fourth bang of $\exp_{\pm 1}$ intersects the fifth bang of $\exp_{\pm 2}$; finally the fourth bang of $\exp_1$ intersects the fourth bang of $\exp_{-1}$ at $T_2 = 0$ and $T_3 = T_{3b}$. See Figure 7.

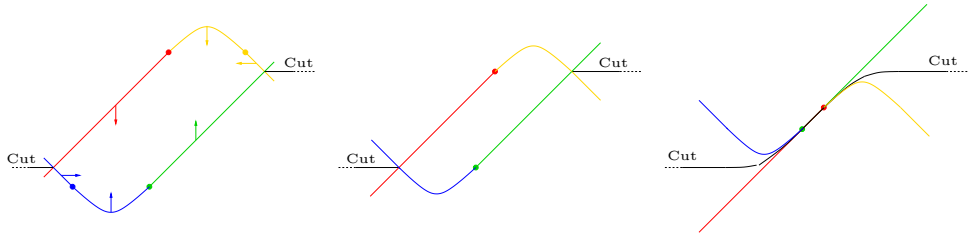

Figure 7: Picture of the front at times with $T_2 = 0$ and $T_3 < T_{3c}$, $T_3 = T_{3c}$ and $T_3 = T_{3b}$

- When $4b_{110} + 8c_{110}c_{200} - 8c_{210} < 0$ and $4b_{110} + 8c_{110}c_{200} - 8c_{210} - 4C_2 > 0$ then the relative position of the two parabola of the fifth bang of $\exp_2$ and $\exp_{-2}$ implies that the sequel of the self intersections of the front is the following : first the fourth bang front of $\exp_{\pm 1}$ intersect the fourth bang front of $\exp_{\pm 2}$; then at time $T_2 = 0$, $T_3 = T_{3c} = T_{3b} + \frac{4}{3}C_2 - \frac{8}{3}c_{110}^2 < T_{3b}$ the fourth bang of $\exp_{\pm 1}$ intersects the fifth bang of $\exp_{\pm 2}$; finally the fifth bang of $\exp_2$ intersects the fifth bang of $\exp_{-2}$ at a time with $T_2 = 0$ and $T_3 = T_{3g}$ between T_{3c} and T_{3b}. See Figure 8.

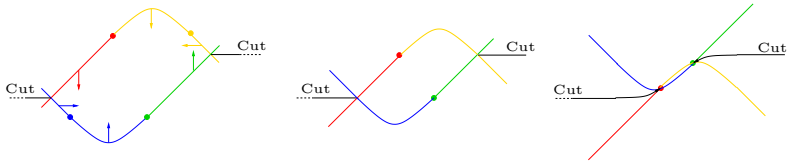

Figure 8: Picture of the front at times with $T_2 = 0$ and $T_3 < T_{3c}$, $T_3 = T_{3c}$ and $T_3 = T_{3g}$

- When $4b_{110} + 8c_{110}c_{200} - 8c_{210} > 0$ and $4b_{110} + 8c_{110}c_{200} - 8c_{210} + 4C_2 < 0$ then the relative position of the two parabola of the fifth bang of $\exp_2$ and $\exp_{-2}$ implies that the sequel of the self intersections of the front is the following : first the fourth bang front of $\exp_{\pm 1}$ intersect the fourth bang front of $\exp_{\pm 2}$; then at time $T_2 = 0$ and $T_3 = T_{3d} = T_{3a} + 2C_2 - 2c_{110}^2 < T_{3a}$

the fourth bang of $\exp_{\pm 2}$ intersects the fifth bang of $\exp_{\mp 2}$; finally the fifth bang of $\exp_2$ intersects the fifth bang of $\exp_{-2}$. The picture is similar to the one of Figure 7.

- When $4b_{110} + 8c_{110}c_{200} - 8c_{210} + 4C_2 > 0$ then all the fifth bang of $\exp_2$ satisfies $x > 4c_{110}\rho^2$ when all the fifth bang of $\exp_{-2}$ satisfies $x < 4c_{110}\rho^2$. This implies that the sequel of the self intersections of the front is the following : first the fourth bang front of $\exp_{\pm 1}$ intersect the fourth bang front of $\exp_{\pm 2}$; then at time $T_2 = 0$ and $T_3 = T_{3d} = T_{3a} + 2C_2 - 2c_{110}^2 < T_{3a}$ the fourth bang of $\exp_{\pm 2}$ intersects the fifth bang of $\exp_{\mp 2}$; finally the fourth bang of $\exp_2$ intersects the fourth bang of $\exp_{-2}$ at $T_2 = 0$ and $T_3 = T_{3a}$. The picture is similar to the one of Figure 8.

In the four cases, the cut locus has only one branch, which is continuous and piecewise smooth. And the proportions are those given in the Figure 9.

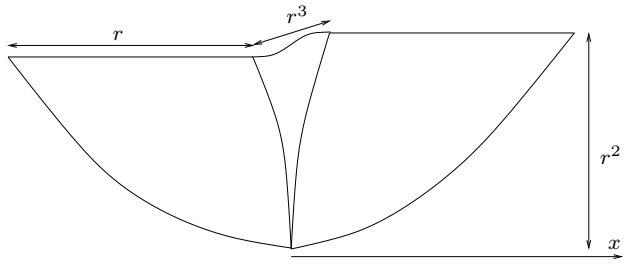

Figure 9: Picture of the cut locus when $C_1 > 0$ and $C_2 < 0$

6.5 Cut locus when $C_1 < 0$ and $C_2 > 0$

The same kind of computations can be done in this case as in the previous case. For the picture of the cut locus we refer to the same figure 8 where the x-axis should be replaced by the y-axis.

6.6 Intersections of fifth bangs

In the case $C_1 < 0$ and $C_2 < 0$, the fifth bang front self intersect before losing optimality. As before this happen for $t \sim 8\rho$ and we write $t = 8\rho + T_2\rho^2 + T_3\rho^3$.

As seen before, each fifth bang front is a part of parabola. For $T_2 < 0$, or $T_2 = 0$ and T_3 small enough, the four parabolas are not intersecting, are positioned as in the figure 10 and they are linked by the part of the front constituted of fourth bangs, and the front do not self intersect.

One way to build the optimal part of the front is to consider the expressions of the fifth bangs and of the four bangs, to consider them for all the values of $\alpha_i \in [-1, 1]$ and to keep only the part which constitutes the boundary of the "central" domain (see Figure 10). The dynamics with respect to T_3 of each of these expressions consist only on translations of $\pm T_3$ along x or y. Hence to identify the optimal part of these expressions, we just have to understand what are the consecutive intersections when T_3 varies.

- The first intersection is of the fifth bang front of $\exp_{\pm 1}$ with the one of $\exp_{\pm 2}$ at $T_2 = 0$ and $T_3 = T_{3e}$ or with the one of $\exp_{\mp 2}$ at $T_2 = 0$ and $T_3 = T_{3f}$.

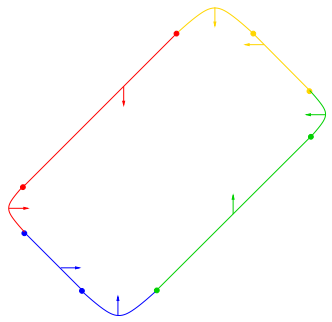

Figure 10: The front before $t = 8\rho$ when $C_1 < 0$ and $C_2 < 0$

When writing the intersection of the fifth fronts, that is for example that $x_{1sus}(\alpha_2 = -1) = x_{2sus}(\alpha_1 = 1)$ and $y_{1sus}(\alpha_2 = -1) = y_{2sus}(\alpha_1 = 1)$, one finds

$$T_{3e} = \frac{4}{3}(a_{110} + 3b_{110} - 6b_{200} + 18c_{110}c_{200} + 2c_{120} + 6c_{300} - 6c_{210})$$

and

$$T_{3f} = \frac{4}{3}(a_{110} - 3b_{110} - 6b_{200} + 6c_{110}c_{200} + 2c_{120} + 6c_{300} + 6c_{210}).$$

After that time, the fifth bang fronts that connected self intersect, until a next event.

Case 1 The next event can be that all the front corresponding to the fifth bang of $\exp_{\pm 1}$ (resp. $\exp_{\pm 2}$) is no more optimal. This comes from the fact that

- the entire arc of parabolas of the fifth bang front of $\exp_{\pm 1}$ crossed the parabolas of $\exp_{\pm 2}$ which occures if $2|C_1| < |C_2|$.
- the entire arc of parabolas of the fifth bang front of $\exp_{\pm 2}$ crossed the parabolas of $\exp_{\pm 1}$ which occures if $2|C_1| > |C_2|$,

see figure 11. The corresponding time can be computed in the following way. Assume that $T_{3e} < T_{3f}$ and hence that the first event was the contact of the fifth bang front of $\exp_1$ with the one of $\exp_2$ at one of their extremity. Then, the second event will happen at T_3 such that one of the other extremities, let call it $q(T_3)$ crosses the other parabola at $p(T_3)$, see Figure FIGURE. Thanks to the dynamics with respect to T_3, $p(T_3)$ and $q(T_3)$ belongs for all T_3 at the line $x + y = c + T_3$ where $c \in \mathbb{R}$. Together with the expressions of the parabolas one find that the corresponding time is $T_3 = T_{3e} + \tau_3$ with

$$\tau_3 = 8\sqrt{2C_1C_2}.$$

If $T_{3f} < T_{3e}$ then it happens at $T_3 = T_{3f} + \tau_3$.

Case 2 An other event, that can occures after the first intersection, is the other contact between fifth bang fronts occures. If $T_{3e} < T_{3f}$ then this event is at $T_3 = T_{3f}$ and if $T_{3f} < T_{3e}$ it is at $T_3 = T_{3f}$. See Figure 12

Case 1.1 In the case 1, the next event can be the closure of the synthesis by the contact of the four bangs. If $T_{3e} < T_{3f}$ the fourth bang fronts of $\exp_1$ and $\exp_{-1}$ can intersect at time T_{3b}. If

$T_{3f} < T_{3e}$ the fourth bang fronts of $\exp_2$ and $\exp_{-2}$ can intersect at time T_{3a}. This case occures only if the arc of parabolas of $\exp_{\pm 1}$ from one part, and the arc of parabolas of $\exp_{\pm 2}$ from the other part, do not intersect at any time T_3.

Case 1.2 In the case 1, another possibility is that the four bang front loses entirely its optimality. If $2|C_1| < |C_2|$ it correspond to the time at which an extremity of the fifth bang front of exp_2 touches the fifth bang front of exp_{-2}. If $2|C_1| > |C_2|$ it correspond to the time at which an extremity of the fifth bang front of exp_1 touches the fifth bang front of exp_{-1}. These times can be computed by translating in the calculus these intersection and we gat in the different cases

- If $T_{3e} < T_{3f}$ and $|C_2| < 2|C_1|$ then $T_3 = T_{3g} = -K_1 + 2C_1(1+\alpha_g^2)$ with $\alpha_g = -1 + \frac{1}{C_1}(b_{110} + 2c_{110}c_{200} - 2c_{210})$ and

$$K_1 = \frac{16}{3}c_{120} - \frac{4}{3}a_{110} - 4c_{110}^2 - 16c_{110}c_{200} - 8c_{200}^2 + 4c_{300}.$$

- If $T_{3e} < T_{3f}$ and $|C_2| > 2|C_1|$ then $T_3 = T_{3h} = -K_2 + 2C_2(1+\alpha_h^2)$ with $\alpha_h = 1 - \frac{2}{C_2}(b_{110} + 2c_{110}c_{200} - 2c_{210})$ and

$$K_2 = \frac{4}{3}c_{120} - \frac{4}{3}a_{110} - 2c_{110}^2 - 16c_{110}c_{200} - 16c_{200}^2 + 16c_{300} - 8b_{200}.$$

- If $T_{3e} > T_{3f}$ and $|C_2| < 2|C_1|$ then $T_3 = T_{3i} = -K_1 + 2C_1(1+\alpha_i^2)$ with $\alpha_i = 1 + \frac{1}{C_1}(b_{110} + 2c_{110}c_{200} - 2c_{210})$.
- If $T_{3e} > T_{3f}$ and $|C_2| > 2|C_1|$ then $T_3 = T_{3j} = -K_2 + 2C_2(1+\alpha_j^2)$ with $\alpha_j = -1 - \frac{2}{C_2}(b_{110} + 2c_{110}c_{200} - 2c_{210})$.

After the fourth bang front lost optimality the optimal synthesis finishes by the last self intersection of the fifth bang front.

Case 2.2 In case two, after $\max\{T_{3e}, T_{3f}\}$, the optimal synthesis closes as follows. If $|C_2| < 2|C_1|$, then the next event is the loss of optimality of the entire fifth bang front of $\exp_{\pm 2}$, and the optimal synthesis finishes by the intersection of the parabolas of $\exp_{\pm 1}$. If $|C_2| > 2|C_1|$, then the next event is the loss of optimality of the entire fifth bang front of $\exp_{\pm 1}$, and the optimal synthesis finishes by the intersection of the parabolas of $\exp_{\pm 2}$

6.7 Cut locus when $C_1 < 0$ and $C_2 < 0$

Thanks to the description of the different steps that can occure along the dynamics of the front, we can conclude by claming

- If $|T_{3e} - T_{3f}| < \tau_3$ then the cut locus has 5 smooth branches as in Figure 12.
- If not it has only one branch which is continuous and smooth by arcs, see Figure 11.

Finally we can give the picture of the cut locus in this two cases in Figure 13.

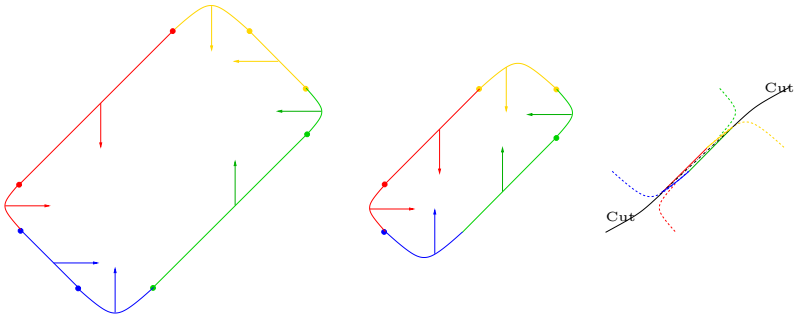

Figure 11: Evolution of the front when $|T_{3e} - T_{3f}| > \tau_3$

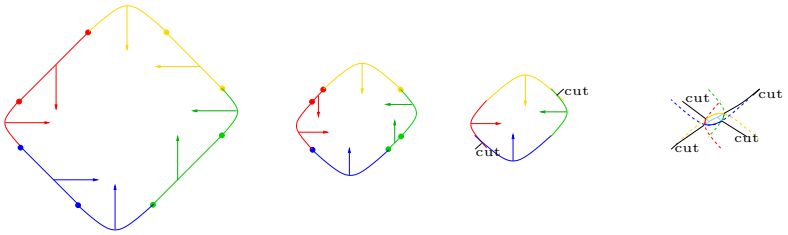

Figure 12: Evolution of the front when $|T_{3e} - T_{3f}| < \tau_3$

6.8 Singularities and stability, open question

All the computations we made in this section for the cut locus or conjugate locus are stable except for extremals with initial conditions $|\lambda_x| = |\lambda_y| = 1$. Effectively, under the codimension 1 assumption that both $C_1 \neq 0$ and $C_2 \neq 0$, except for these initial conditions, the cut points correspond to transversal self intersections of the wave front.

For the initial conditions $|\lambda_x| = |\lambda_y| = 1$, a further study should be done in order to find a good notion of stability, which is itself not clear, and to study it in this case. In the case $C_1 > 0$ and $C_2 > 0$, the corresponding singularity in the sub-Riemannian contact case, corresponding to the extremity of the cut locus, is a cusp $\mathcal{A}_3$ (in the classification of Arnol'd) and it is stable as smooth or lagrangian singularity. We may propose the conjecture that a good theory of stability should find in our context that the singularity is stable. If this conjecture is valid then the pictures of the cut locus are stable and valid not only for the jet of the dynamics we have computed but also for the true dynamics.

7 Extremals with only one control switching several times

For $|\lambda_z|$ large enough the dynamics is described in the previous sections. We can now choose a constant $\Lambda_z > 0$ large enough and considering only the extremal satisfying $|\lambda_z| < \Lambda_z$. As seen before, along an extremal

$$\dot{\phi}_3 \quad = \quad u_1(f_{41}\phi_1 + f_{42}\phi_2 + f_{43}\phi_3) + u_2(f_{51}\phi_1 + f_{52}\phi_2 + f_{53}\phi_3).$$

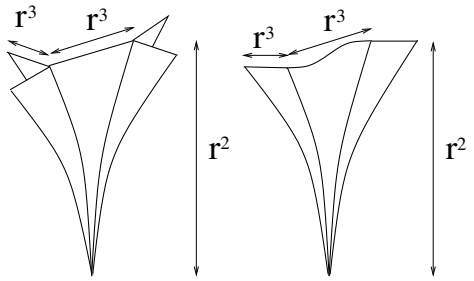

Figure 13: Possible cut loci when $C_1 < 0$ and $C_2 < 0$

One computes easily that

$$\begin{array}{ll} f_{41} = -\frac{a_{110}+2a_{200}+b_{110}+2b_{200}}{4}, & f_{51} = \frac{a_{110}-2a_{200}+b_{110}-2b_{200}}{4}, \\ f_{42} = -\frac{a_{110}+2a_{200}-b_{110}-2b_{200}}{4}, & f_{52} = \frac{a_{110}-2a_{200}-b_{110}+2b_{200}}{4}, \\ f_{43} = \frac{1}{2}c_{110} + c_{200}, & f_{53} = -\frac{1}{2}c_{110} + c_{200}. \end{array}$$

With $|\phi_1| \leq 1$ and $|\phi_2| \leq 1$, we get

$$|\dot{\phi}_3| \leq |f_{41}| + |f_{42}| + |f_{51}| + |f_{52}| + (|f_{53}| + |f_{43}|)|\phi_3| \leq 4M' + 2M'\Lambda_z$$

where M' is a local bound of the f_{ij}. This implies that, for the extremals we are considering, the possibility of switching in short time implies that the corresponding switching function starts close to 0. Which implies that in short time only one control switches. And if in short time a control switches twice hence ϕ_3 should change sign and hence starts close to 0 that is λ_z should starts close to 0.

In the following, we will be interested only in finding extremals that switch at least twice (on the same control) since the ones that switch only once are yet obtained with initial conditions with large $|\lambda_z|$.

We will consider only extremals with $u_1 \equiv 1$, the study of the other ones being equivalent. Along such an extremal

$$\ddot{\phi}_2 = u_1\dot{\phi}_3 = \dot{\phi}_3$$

and since $u_1 \equiv 1$ one gets

$$\ddot{\phi}_2 = (f_{41} + u_2 f_{51})\phi_1 + (f_{42} + u_2 f_{52})\phi_2 + (f_{43} + u_2 f_{53})\phi_3.$$

Since $\phi_3(t) = O(t)$, $\phi_2 = O(t)$ and $\phi_1(t) = 1 + O(t)$ we get that

$$\ddot{\phi}_2(t) = (f_{41} + u_2 f_{51}) + O(t).$$

In the following we assume that we are considering a point where $f_{41} + f_{51} \neq 0$ and $f_{41} - f_{51} \neq 0$. We consider then the four following cases

1. If $|f_{51}| < f_{41}$ then $f_{41} + u_2 f_{51} > 0$ for all $u_2 \in [0, 1]$ and $\ddot{\phi}_2(t) > 0$ for all t. As a consequence the only possible behaviours of the control u_2 are (see Figure 14)

   (a) $u_2 \equiv 1$,

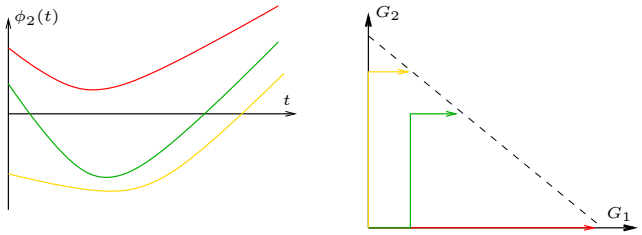

Figure 14: Extremals when $|f_{51}| < f_{41}$

(b) $u_2 = -1$ during a first intervalle of time and switches to 1,

(c) $u_2 = 1$ during a first intervalle of time, then -1 during a second one, and finally switches to 1.

2. If $|f_{51}| < -f_{41}$ then $f_{41} + u_2 f_{51} < 0$ for all $u_2 \in [0, 1]$ and $\ddot{\phi}_2(t) < 0$ for all t. As a consequence the only possible behaviours of the control u_2 are (see Figure 15)

   (a) $u_2 \equiv -1$,

   (b) $u_2 = 1$ during a first intervalle of time and switches to -1,

   (c) $u_2 = -1$ during a first intervalle of time, then 1 during a second one, and finally switches to -1.

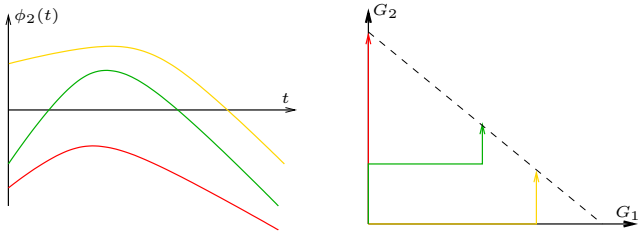

Figure 15: Extremals when $|f_{51}| < -f_{41}$

3. If $|f_{41}| < f_{51}$ then $f_{41} + f_{51} > 0$ hence $\ddot{\phi}_2(t) > 0$ when $\phi_2(t) > 0$ and $f_{41} - f_{51} < 0$ hence $\ddot{\phi}_2(t) < 0$ when $\phi_2(t) < 0$. In that case the possible behaviours of the control u_2 are (see Figure 16)

   (a) u_2 is constant and equal to ± 1,

   (b) u_2 is equal to 1 or -1 during a first intervalle of time and switches to -1 or 1,

   (c) u_2 is equal to 1 or -1 during a first intervalle of time, then $\phi_2 = 0$ during a second intervalle where $u_2(t) = -\frac{f_{41}(q(t))}{f_{51}(q(t))} + O(t)$, and finally u_2 switches to 1 or -1.

4. If $|f_{41}| < -f_{51}$ then $f_{41} + f_{51} < 0$ hence $\ddot{\phi}_2(t) < 0$ when $\phi_2(t) > 0$ and $f_{41} - f_{51} > 0$ hence $\ddot{\phi}_2(t) > 0$ when $\phi_2(t) < 0$. In that case the list of possible behaviours may be very large. In the following we analyse more deeply to prove that the possible behaviours are

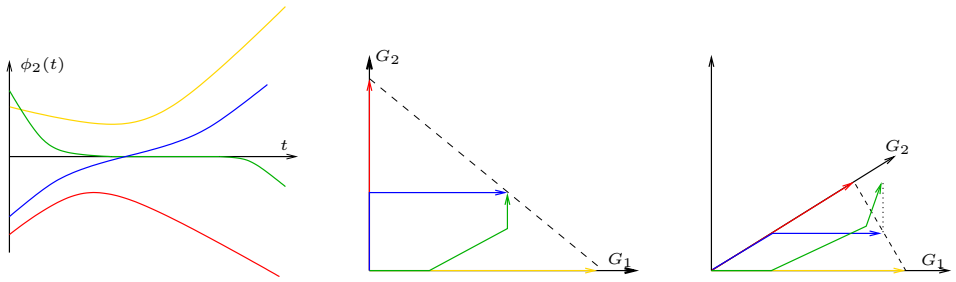

Figure 16: Extremals when $|f_{41}| < f_{51}$

(a) u_2 is constant and equal to ± 1,

(b) u_2 is constant and equal to ± 1 during a first intervalle of time and switches to ∓ 1,

(c) u_2 is constant and equal to ± 1 during a first intervalle of time and switches to ∓ 1, and finally switches again to ± 1.

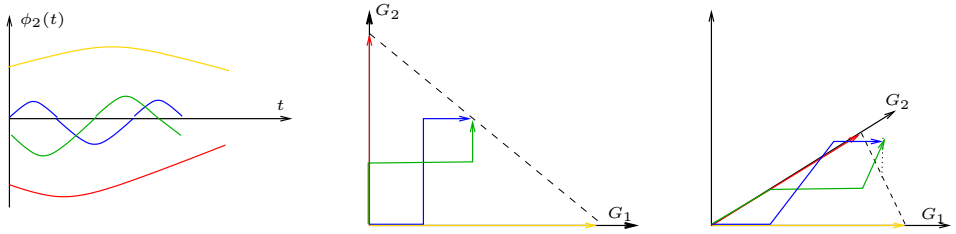

Figure 17: Extremals when $|f_{41}| < -f_{51}$

A more precise description of the optimal ones is given in the following analysis. In particular, in this case, appears a cut locus.

7.1 Extremals when $|f_{41}| < -f_{51}$

In the following we prove that, in the case $|f_{41}| < -f_{51}$, an extremal with $u_1 \equiv 1$ with four bangs is not optimal.

An easy computation shows that

$$\begin{aligned} f_{41}(0) &= -\frac{1}{2}(a_{200} + b_{200} + \frac{a_{110} + b_{110}}{2}) \\ f_{51}(0) &= -\frac{1}{2}(a_{200} + b_{200} - \frac{a_{110} + b_{110}}{2}) \end{aligned}$$

The hypothesis $|f_{41}| < -f_{51}$ is equivalent to $a_{200} + b_{200} > 0$ and $\frac{a_{110}+b_{110}}{2} < 0$.

Consider the three following extremals from $(0,0,0)$ to (x,y,z). The first one, denoted ϵ, has $u_2 = 1$ during time ϵ_1 then $u_2 = -1$ during time ϵ_2 and finally $u_2 = 1$ during time ϵ_3. The second one, denoted $\theta(t)$, has $u_2 = -1$ during time θ_1 then $u_2 = 1$ during time θ_2 and finally $u_2 = -1$ during time θ_3. The last one, denoted $\gamma(t)$, has $u_2 = -1$ during time γ_1 then $u_2 = 1$ during time

γ_2 then $u_2 = -1$ during time γ_3 and finally $u_2 = 1$ during time γ_4. One prove easily that, denoting $s_\epsilon = \epsilon_1 + \epsilon_2 + \epsilon_3$, $s_\theta = \theta_1 + \theta_2 + \theta_3$ and $s_\gamma = \gamma_1 + \gamma_2 + \gamma_3 + \gamma_4$,

$$\begin{aligned} x_\epsilon(s_\epsilon) &= \epsilon_1 + \epsilon_3 + a_{200}\epsilon_1^2\epsilon_2 + a_{110}\epsilon_1\frac{\epsilon_2^2}{2} + o(s_\epsilon^3), \\ y_\epsilon(s_\epsilon) &= \epsilon_2 + b_{200}\epsilon_1^2\epsilon_2 + b_{110}\epsilon_1\frac{\epsilon_2^2}{2} + o(s_\epsilon^3), \\ z_\epsilon(s_\epsilon) &= \epsilon_1\epsilon_2 + o(s_\epsilon^2), \end{aligned}$$

$$\begin{aligned} x_\theta(s_\theta) &= \theta_2 + a_{200}\theta_2^2\theta_3 + a_{110}\theta_2\theta_3(\theta_1 + \frac{\theta_3}{2}) + o(s_\theta^3), \\ y_\theta(s_\theta) &= \theta_1 + \theta_3 + b_{200}\theta_2^2\theta_3 + b_{110}\theta_2\theta_3(\theta_1 + \frac{\theta_3}{2}) + o(s_\theta^3), \\ z_\theta(s_\theta) &= \theta_2\theta_3 + o(s_\theta^2), \end{aligned}$$

$$\begin{aligned} x_\gamma(s_\gamma) &= \gamma_2 + \gamma_4 + a_{200}\gamma_2^2\gamma_3 + a_{110}\gamma_2\gamma_3(\gamma_1 + \frac{\gamma_3}{2}) + o(s_\gamma^3), \\ y_\gamma(s_\gamma) &= \gamma_1 + \gamma_3 + b_{200}\gamma_2^2\gamma_3 + b_{110}\gamma_2\gamma_3(\gamma_1 + \frac{\gamma_3}{2}) + o(s_\gamma^3), \\ z_\gamma(s_\gamma) &= \gamma_2\gamma_3 + o(s_\gamma^2), \end{aligned}$$

but since at s_θ and s_γ the extremals are supposed to be at (x, y, z) then one gets

$$\begin{aligned} x + y &= s_\theta + (a_{200} + b_{200})\theta_2^2\theta_3 + \frac{a_{110} + b_{110}}{2}\theta_2\theta_3(\theta_1 + \frac{\theta_3}{2}) + o_(s_\theta^3) \\ &= s_\theta + (a_{200} + b_{200})\theta_2 z + \frac{a_{110} + b_{110}}{2}z(2\theta_1 + \theta_3) \\ x + y &= s_\gamma + (a_{200} + b_{200})\gamma_2^2\gamma_3 + \frac{a_{110} + b_{110}}{2}\gamma_2\gamma_3(\gamma_1 + \frac{\gamma_3}{2}) + o_(s_\gamma^3) \\ &= s_\gamma + (a_{200} + b_{200})\gamma_2 z + \frac{a_{110} + b_{110}}{2}z(2\gamma_1 + \gamma_3). \end{aligned}$$

Hence we deduce

$$\begin{aligned} \frac{s_\gamma - s_\theta}{z} &= (a_{200} + b_{200})(\theta_2 - \gamma_2) + \frac{a_{110} + b_{110}}{2}(2\theta_1 + \theta_3 - (2\gamma_1 + \gamma_3)) + o(x + y) \\ &= (a_{200} + b_{200})(\theta_2 - \gamma_2) + \frac{a_{110} + b_{110}}{2}(\theta_1 - \gamma_1) + o(x + y) \end{aligned}$$

since $\theta_1 + \theta_3 = y + o(x + y)$ and $\gamma_1 + \gamma_3 = y + o(x + y)$.

Now, we should analyse the relation between γ_2 and γ_3. One can prove that along the curve γ, during the second bang, $\ddot{\phi}_2 = f_{41} - f_{51} + o(t) = -\frac{a_{110}+b_{110}}{2} + o(t)$ and during the second bang $\ddot{\phi}_2 = f_{41} + f_{51} + o(t) = -(a_{200} + b_{200}) + o(t)$. One proves easily that, since $\phi_2 = 0$ at the extremity of each of these intervalles, this implies that

$$\frac{\gamma_3}{\gamma_2} = -\frac{a_{200} + b_{200}}{\frac{a_{110}+b_{110}}{2}} + o(x + y),$$

hence exists $\lambda > 0$ such that $\gamma_3 = \lambda(a_{200} + b_{200}) + o((x+y)^2)$ and $\gamma_2 = -\lambda\frac{a_{110}+b_{110}}{2} + o((x+y)^2)$. As a consequence

$$\begin{aligned}
\lambda\frac{s_\gamma - s_\theta}{z} &= \gamma_3(\theta_2 - \gamma_2) - \gamma_2(\theta_1 - \gamma_1) + o((x+y)^2) \\
&= \gamma_3(x - \gamma_2) - \gamma_2(\gamma_3 - \theta_3) + o((x+y)^2) \\
&= \gamma_3 x + \gamma_2\frac{z}{x} - 2\gamma_2\gamma_3 + o((x+y)^2) \\
&= \gamma_3 x + \frac{z}{\gamma_3}\frac{z}{x} - 2z + o((x+y)^2)
\end{aligned}$$

hence

$$\lambda\frac{s_\gamma - s_\theta}{z^2} = \frac{\gamma_3 x}{z} + \frac{z}{x\gamma_3} - 2 + o(1)$$

hence $s_\gamma - s_\theta$ is strictly positive except maybe when $\gamma_3 \sim \theta_3$ and $\gamma_2 \sim x$.

But comparing with the curve ϵ we get that $s_\gamma - s_\epsilon > 0$ except maybe when $\gamma_2 \sim \epsilon_1$ and $\gamma_3 \sim y$. Finally we can conclude that such an extremal γ is not optimal. The same proof can be done for the extremals with four bangs following first G_1, then G_2, then G_1 and finally G_2. And no extremal with three switches on the same control can be optimal.

Comparing the curves ϵ and θ one gets

$$\frac{s_\epsilon - s_\theta}{z(1 - \frac{z}{xy})} = (a_{200} + b_{200})x + \frac{a_{110} + b_{110}}{2}y + o(x+y).$$

Hence, since $a_{200} + b_{200} > 0$ and $\frac{a_{110}+b_{110}}{2} < 0$ the curve ϵ is optimal for $y > -2\frac{a_{200}+b_{200}}{a_{110}+b_{110}}x + o(x)$ and we find that there is a cut locus which is tangent at 0 to the plane

$$(a_{200} + b_{200})x + \frac{a_{110} + b_{110}}{2}y = 0.$$

7.2 Other extremals generating cut locus

One show easily that, for extremals with $u_1 \equiv 1$, there is also cut locus only if $|f_{41}| < -f_{51}$, that is if $a_{200} + b_{200} > 0$ and $a_{110} + b_{110} < 0$, and the tangent plane is the same.

In the cases $u_2 \equiv 1$ and $u_2 \equiv -1$ then there is cut locus only if $|f_{52}| < f_{42}$, that is if $b_{110} - a_{110} > 0$ and $b_{200} - a_{200} > 0$. In this last case the tangent plane at 0 is

$$(a_{200} - b_{200})x + \frac{a_{110} - b_{110}}{2}y = 0.$$

7.3 Cut locus generated by extremals with $\lambda_z(0) \sim 0$

As a consequence of the previous computations, we can describe the part of the local cut locus generated by the extremals with $\lambda_0(0) \sim 0$.

- if ($a_{200} + b_{200} < 0$ or $a_{110} + b_{110} > 0$) and ($b_{110} - a_{110} < 0$ or $b_{200} - a_{200} < 0$) then this part of the local cut locus is empty.
- if $a_{200} + b_{200} > 0$ and $a_{110} + b_{110} < 0$ and ($b_{110} - a_{110} < 0$ or $b_{200} - a_{200} < 0$) then this part of the cut locus writes

$$\{(x, -2\frac{a_{200} + b_{200}}{a_{110} + b_{110}}x + o(x), z) \mid 0 \leq z \leq -2\frac{a_{200} + b_{200}}{a_{110} + b_{110}}x^2 + o(x^2)\}$$

- if ($a_{200} + b_{200} < 0$ or $a_{110} + b_{110} > 0$) and $b_{110} - a_{110} > 0$ and $b_{200} - a_{200} > 0$ then this part of the cut locus writes

$$\{(x, -2\frac{a_{200} - b_{200}}{a_{110} - b_{110}}x + o(x), z) \mid 0 \geq z \geq -2\frac{a_{200} - b_{200}}{a_{110} - b_{110}}x^2 + o(x^2)\}$$

- if $a_{200} + b_{200} > 0$ and $a_{110} + b_{110} < 0$ and $b_{110} - a_{110} > 0$ and $b_{200} - a_{200} > 0$ then this part of the local cut locus is the union of the two previous sets.

Finally we can propose the picture of this part of the cut locus in Figure 18

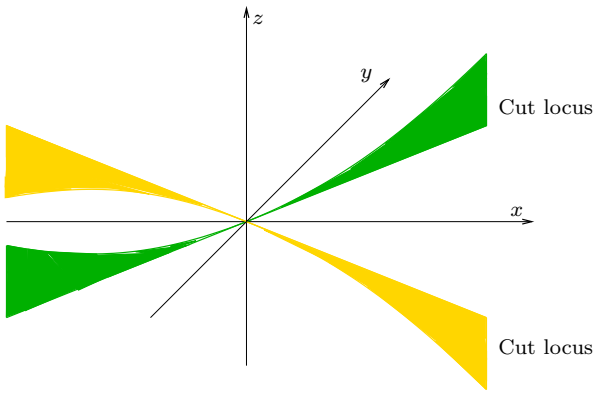

Figure 18: Part of the cut locus generated by the extremal with $\lambda_z(0) \sim 0$ when $|f_{41}| < -f_{51}$ and $|f_{52}| < f_{42}$

References

[1] A. Agrachev, B. Bonnard, M. Chyba, and I. Kupka. Sub-Riemannian sphere in Martinet flat case. *ESAIM Control Optim. Calc. Var.*, 2:377–448, 1997.

[2] A. A. Agrachev, U. Boscain, G. Charlot, R. Ghezzi, and M. Sigalotti. Two-dimensional almost-Riemannian structures with tangency points. *Ann. Inst. H. Poincaré Anal. Non Linéaire*, 27(3):793–807, 2010.

[3] A. A. Agrachev, El-H. Chakir El-A., and J. P. Gauthier. Sub-Riemannian metrics on $\mathbf{R}^3$. In *Geometric control and non-holonomic mechanics (Mexico City, 1996)*, volume 25 of *CMS Conf. Proc.*, pages 29–78. Amer. Math. Soc., Providence, RI, 1998.

[4] Andrei Agrachev and Jean-Paul Gauthier. On the subanalyticity of Carnot-Caratheodory distances. *Ann. Inst. H. Poincaré Anal. Non Linéaire*, 18(3):359–382, 2001.

[5] Andrei A. Agrachev and Yuri L. Sachkov. *Control theory from the geometric viewpoint*, volume 87 of *Encyclopaedia of Mathematical Sciences*. Springer-Verlag, Berlin, 2004. Control Theory and Optimization, II.

[6] E. Ali and G. Charlot. Local (sub) finslerian geometry for the maximum norm in dimension 2. *preprint*.

[7] D. Barilari, U. Boscain, E. Le Donne, and M. Sigalotti. Sub-finsler structures from the time-optimal control viewpoint for some nilpotent distributions. *arXiv:1506.04339*, 2016.

[8] Davide Barilari, Ugo Boscain, Grégoire Charlot, and Robert W. Neel. On the heat diffusion for generic riemannian and sub-riemannian structures. *IMRN*, 2016.

[9] Davide Barilari, Ugo Boscain, and Robert W. Neel. Small-time heat kernel asymptotics at the sub-Riemannian cut locus. *J. Differential Geom.*, 92(3):373–416, 2012.

[10] André Bellaïche. The tangent space in sub-Riemannian geometry. In *Sub-Riemannian geometry*, volume 144 of *Progr. Math.*, pages 1–78. Birkhäuser, Basel, 1996.

[11] G. Ben Arous. Développement asymptotique du noyau de la chaleur hypoelliptique hors du cut-locus. *Ann. Sci. École Norm. Sup. (4)*, 21(3):307–331, 1988.

[12] G. Ben Arous and R. Léandre. Décroissance exponentielle du noyau de la chaleur sur la diagonale. II. *Probab. Theory Related Fields*, 90(3):377–402, 1991.

[13] B. Bonnard, M. Chyba, and E. Trelat. Sub-riemannian geometry, one-parameter deformation of the martinet flat case. *J. Dyn. Control Syst. 4, No.1, 59-76 (1998).*, 4:59–76, 1998.

[14] Bernard Bonnard, Grégoire Charlot, Roberta Ghezzi, and Gabriel Janin. The Sphere and the Cut Locus at a Tangency Point in Two-Dimensional Almost-Riemannian Geometry. *J. Dynam. Control Systems*, 17(1):141–161, 2011.

[15] Bernard Bonnard and Monique Chyba. Méthodes géométriques et analytiques pour étudier l'application exponentielle, la sphère et le front d'onde en géométrie sous-riemannienne dans le cas Martinet. *ESAIM Control Optim. Calc. Var.*, 4:245–334 (electronic), 1999.

[16] U. Boscain, G. Charlot, and R. Ghezzi. Normal forms and invariants for 2-dimensional almost-Riemannian structures. *Differential Geom. Appl.*, 31(1):41–62, 2013.

[17] U. Boscain, G. Charlot, R. Ghezzi, and M. Sigalotti. Lipschitz classification of almost-riemannian distances on compact oriented surfaces. *Journal of Geometric Analysis*, pages 1–18. 10.1007/s12220-011-9262-4.

[18] Ugo Boscain, Thomas Chambrion, and Grégoire Charlot. Nonisotropic 3-level quantum systems: complete solutions for minimum time and minimum energy. *Discrete Contin. Dyn. Syst. Ser. B*, 5(4):957–990, 2005.

[19] E. Breuillard and E. Le Donne. On the rate of convergence to the asymptotic cone for nilpotent groups and subfinsler geometry. *Proc. Natl. Acad. Sci. USA*, 110(48):19220–19226, 2013.

[20] Grégoire Charlot. Quasi-contact s-r metrics : normal form in $\mathbb{R}^{2n}$, wave front and caustic in $\mathbb{R}^4$. *Acta App. Math.*, 74:217–263, 2002.

[21] W. L. Chow. ber systeme von linearen partiellen differentialgleichungen erster ordnung. *Math. Ann.*, 117:98–105, 1939.

[22] Jeanne Clelland and Christopher Moseley. Sub-finsler geometry in dimension three. *Differ. Geom. Appl.*, 24(6):628–651, 2006.

[23] Jeanne Clelland, Christopher Moseley, and George Wilkens. Geometry of sub-finsler engel manifolds. *Asian J. Math.*, 11(4):699–726, 2007.

[24] El-Houcine Chakir El Alaoui, J.-P. Gauthier, and I. Kupka. Small sub-riemannian balls on $\mathbb{R}^3$. *J. Dyn. Control Syst.*, 2(3):359–421, 1996.

[25] A.F. Filippov. On some questions in the theory of optimal regulation: existence of a solution of the problem of optimal regulation in the class of bounded measurable functions. *Vestnik Moskov. Univ. Ser. Mat. Meh. Astr.Fiz.Him.*, 2:2532, 1959.

[26] Rémi Léandre. Majoration en temps petit de la densité d'une diffusion dégénérée. *Probab. Theory Related Fields*, 74(2):289–294, 1987.

[27] Rémi Léandre. Minoration en temps petit de la densité d'une diffusion dégénérée. *J. Funct. Anal.*, 74(2):399–414, 1987.

[28] P.K. Rashevsky. About connecting two points of complete nonholonomic space by admissible curve. *Uch. Zap. Ped. Inst. Libknehta*, 2:83–94, 1938.

[29] M. Sigalotti. Some computations for 2nd variations in sub-finsler geometry. *preprint*.